

LARGE-SCALE BIOLOGY ARTICLE

Induced Genome-Wide Binding of Three Arabidopsis WRKY Transcription Factors during Early MAMP-Triggered Immunity

Rainer P. Birkenbihl, Barbara Kracher and Imre E. Somssich*

Department of Plant Microbe Interactions, Max Planck Institute for Plant Breeding Research, Carl-von-Linné Weg 10, 50829 Koeln, Germany

*Corresponding author: somssich@mpipz.mpg.de

Short title: WRKY Factors in MAMP-triggered Immunity

One-sentence summary: Genome-wide analysis reveals the *in vivo* binding sites of Arabidopsis WRKY18, WRKY33 and WRKY40 transcription factors during early MTI and the consequences of WRKY18 and WRKY40 binding on transcriptional output.

The author responsible for distribution of materials integral to the findings presented in this article in accordance with the policy described in the Instructions for Authors is: Imre E. Somssich (somssich@mpipz.mpg.de).

ABSTRACT

During microbial-associated molecular pattern (MAMP)-triggered immunity (MTI) molecules derived from microbes are perceived by cell surface receptors and upon signaling to the nucleus initiate a massive transcriptional reprogramming critical to mount an appropriate host defense response. WRKY transcription factors play an important role in regulating these transcriptional processes. Here, we determined on a genome-wide scale the flg22-induced *in vivo* DNA-binding dynamics of three of the most prominent WRKY factors, WRKY18, WRKY40 and WRKY33. The three WRKY factors each bound to more than 1000 gene loci predominantly at W-box elements, the known WRKY binding motif. Binding occurred mainly in the 500 bp promoter regions of these genes. Many of the targeted genes are involved in signal perception and transduction not only during MTI but also upon damage-associated molecular pattern (DAMP)-triggered immunity (DTI), providing a mechanistic link between these functionally interconnected basal defense pathways. Among the additional targets were genes involved in the production of indolic secondary metabolites and in modulating distinct plant hormone pathways. Importantly, among the targeted genes were numerous transcription factors, encoding predominantly ethylene response factors, active during early MTI, and WRKY factors, supporting the previously hypothesized existence of a WRKY sub-regulatory network. Transcriptional analysis revealed that WRKY18 and WRKY40 function redundantly as negative regulators of flg22-induced genes often to prevent exaggerated defense responses.

37 Introduction

38 Plants are constantly exposed to a wide range of pathogens in their environment but owing to
39 their intricate and efficient basal defense system can often ward off such threats. Key to this
40 successful defense is the ability of plants to recognize various conserved microbial structures,
41 termed microbe-associated molecular patterns (MAMPs), through dedicated plasma
42 membrane-localized pattern recognition receptors (PRRs), and to rapidly initiate intracellular
43 signaling leading to MAMP-triggered immunity (MTI) (Monaghan and Zipfel, 2012;
44 Schwessinger and Ronald, 2012; Newman et al., 2013; Vidhyasekaran, 2014; Li et al., 2016).
45 FLS2 is currently the most intensively studied Arabidopsis PRR and is activated upon binding
46 of bacterial flagellin or flg22, which is a conserved epitope present in the flagellin N-terminus
47 (Zipfel et al., 2004; Sun et al., 2013; Kadota et al., 2014). Upon flg22 perception, several
48 immediate host responses can be observed including the influx of H^+ and Ca^{2+} , the generation
49 of reactive oxygen species (ROS), and the activation of calcium-dependent protein kinases and
50 MAP kinase cascades (Vidhyasekaran, 2014). Subsequently, as with other ligand-PRR
51 interactions, binding of flg22 to FLS2 results in rapid and massive transcriptional
52 reprogramming within the host cell (Zipfel et al., 2004; Zipfel et al., 2006; Wan et al., 2008).

53 Transcriptional profiling has revealed that the expression of thousands of host genes is
54 significantly altered during MTI. Wildtype Arabidopsis seedlings treated for 30-60 min with flg22
55 showed altered expression of more than 1000 genes and a rapid induction of gene sets
56 classified to be involved in signal perception, signal transduction and transcriptional regulation
57 (Navarro et al., 2004; Zipfel et al., 2004). Prominent among the transcription factor (TF) genes
58 that were induced by flg22 early on during MTI are members of the WRKY TF family. Fifteen
59 WRKY TF genes were already strongly (> 4-fold) induced 30 min post flg22 treatment in
60 Arabidopsis seedlings including *WRKY18* (>10-fold), *WRKY33* (>15-fold), and *WRKY40* (>20-
61 fold) (Zipfel et al., 2004). These latter three WRKYs were also identified to be important
62 functional HUBs within a proposed WRKY regulatory network (Choura et al., 2015). The
63 potential importance of WRKY factors in modulating early MTI responses was further
64 supported by the analysis of promoter sequences of flg22-induced genes, which revealed an
65 over-representation of the W-box *cis*-acting DNA element, the consensus binding site of WRKY
66 TFs (Navarro et al., 2004). Similarly, the W-box was over-represented within promoters of the
67 large group of early flg22-induced receptor-like kinase (RLK) genes (Zipfel et al., 2004).

WRKY factors have been demonstrated to fulfill essential regulatory functions to modulate pathogen-triggered cellular responses in numerous plant species (Rushton et al., 2010; Tsuda and Somssich, 2015). For instance, Arabidopsis WRKY33 is a key positive regulator of resistance against the necrotrophic fungi *Alternaria brassicicola* and *Botrytis cinerea* (Zheng et al., 2006; Birkenbihl et al., 2012). WRKY33 indirectly interacts with MAP kinase 4 via the VQ motif-containing protein MKS1. Upon flg22 treatment WRKY33 is released from this complex and subsequently is associated with the promoter of the camalexin biosynthetic gene *PAD3* (Qiu et al., 2008). Arabidopsis WRKY18 and WRKY40 act redundantly in negatively regulating resistance towards the obligate hemi-biotrophic fungus *Golovinomyces orontii* (Pandey et al., 2010). Genetic studies on these two TFs have also clearly demonstrated that they have dual functions namely acting as negative regulators of MTI, and as positive regulators of effector-triggered immunity mediated by the major resistance gene *RPS4*, and in resistance towards the herbivore *Spodoptera littoralis* (Xu et al., 2006; Lozano-Durán et al., 2013; Schön et al., 2013; Schweizer et al., 2013).

Recently, we succeeded in using ChIP-seq to identify genome-wide binding sites of WRKY33 following infection of mature Arabidopsis leaves with the fungus *B. cinerea* 2100 (Liu et al., 2015). In this study, we aimed to define the genome-wide binding patterns of WRKY 18, WRKY40, and WRKY33 during early MTI in Arabidopsis seedlings treated with the potent MAMP flg22, and to determine the consequence of the observed TF binding on the transcriptional output of the identified target genes.

RESULTS AND DISCUSSION

The function of transcription factors is mainly determined by the genomic sites they bind to and by the genes they regulate. Therefore, to investigate the function of WRKY18, WRKY40 and WRKY33 in early MTI, we determined genome-wide binding sites for those TFs upon flg22 treatment. For ChIP-seq we used transgenic complementation lines of WRKY18 (WRKY18-HA), WRKY40 (WRKY40-HA) and WRKY33 (WRKY33-HA), which expressed the HA-epitope tagged WRKY proteins under control of their native promoters in the respective knockout mutants (see Materials and Methods). In this way, we could avoid the problem that no appropriate antibodies exist against these WRKY factors, and were able to use the same anti-

98 HA antibody to determine the respective protein levels and to isolate proteo-DNA complexes
99 containing the three WRKY proteins. Moreover, it was possible to use wildtype (WT) plants as
100 negative controls, which are genotypically similar to the complementation lines and express the
101 investigated *WRKY* genes without the HA-tag. To induce MTI and achieve a highly
102 synchronous response to the elicitor, which is a precondition for the sensitive and clear
103 detection of binding sites, we grew seedlings in liquid medium and treated them with the
104 bacterial flagellin-derived peptide flg22 (Felix et al., 1999).

105 To investigate *WRKY18*, *WRKY40* and *WRKY33* expression and inducibility at the RNA level,
106 WT seedlings were treated with 1 μ M flg22 and samples taken for qRT-PCR analysis, either
107 untreated or at 1 h, 2 h and 4 h post treatment. All three *WRKY* genes were induced after 1 h
108 flg22 treatment (Figure 1A). While *WRKY18* was constitutively expressed with a moderate
109 flg22-dependent increase at 1 h post treatment, *WRKY40* and *WRKY33* were strongly induced
110 at 1 h with elevated RNA levels observed up to the 4 h time point.

111 Flg22-induced HA-tagged WRKY protein accumulation in the complementation lines followed
112 the RNA expression patterns with a short delay (Figure 1B). For *WRKY18*, significant amounts
113 of protein were visible in the non-induced state, the peak of protein abundance was at 1.5 h,
114 and afterwards the protein level stayed high up to the 6 h time point. A second lower molecular
115 weight protein band was consistently detected at all time points and was very likely a
116 consequence of constant protein degradation in the plants. For *WRKY40* and *WRKY33*, only
117 very low protein levels were detected without elicitation. Upon flg22 treatment, their protein
118 abundance strongly increased with peaks at 3 h and 2 h post elicitation, respectively. Based on
119 the kinetics of protein accumulation, the 2 h time point after flg22 treatment was chosen to
120 determine early MTI-induced WRKY binding sites by ChIP-seq.

121

122 **Analysis of *WRKY18*, *WRKY40* and *WRKY33* binding sites**

123 In the course of this study we established comprehensive lists of genome-wide binding sites for
124 the three WRKY factors, *WRKY18*, *WRKY40* and *WRKY33*, which provide a valuable source of
125 information about general genome-wide in vivo W-box occupancy by WRKY factors, the
126 inducibility of binding elicited by flg22, and genome-wide experimental evidence for the
127 hypothesized WRKY regulatory network (Eulgem, 2006; Eulgem and Somssich, 2007; Chi et

128 al., 2013; Choura et al., 2015). For our ChIP-seq experiments we analyzed material from the
129 three WRKY complementation lines before (0 h) and 2 h after flg22 treatment using the
130 corresponding non-HA-antigen-containing WT plants as negative control.

131 DNA-binding sites in each WRKY-HA line were determined separately for two biological
132 replicates by comparing their observed sequencing read distribution with that of the similarly
133 treated WT sample. Binding sites were scored as reproducible if the corresponding peak region
134 overlapped with a peak region in the other replicate by at least 50 % of the length of the smaller
135 peak region. Furthermore, a binding site in the pooled samples of both replicates was counted
136 as consistent if its peak region overlapped with a reproducible peak region in both of the
137 original replicates by at least 50 % of the length of the smaller region.

138 After 2 h of flg22 treatment, 1403 consistent binding sites were detected for WRKY18, 1622 for
139 WRKY40, and 1208 binding sites for WRKY33 (Supplemental Data Set 1). Since many gene
140 loci contained more than one binding site, the number of predicted target genes was lower,
141 namely 1290 for WRKY18, 1478 for WRKY40 and 1140 for WRKY33 (Table 1). For WRKY40
142 and WRKY33, the observed binding was almost exclusively dependent on flg22 treatment,
143 while for WRKY18 binding to only 380 genes was defined as solely flg22-dependent. This was
144 probably due to the detected constitutive protein levels in the WRKY18 complementation line,
145 which appeared to also reflect the true situation, since elevated *WRKY18* RNA levels were also
146 observed prior to induction by flg22 in WT plants under our tested conditions (Figure 1A).
147 Nevertheless, manual inspection of binding sites using the Integrative Genomics Viewer (IGV;
148 Thorvaldsdóttir et al., 2013) revealed that most of the WRKY18_binding peaks visible at 0 h
149 were significantly higher upon flg22 treatment. We found that half of the 209 consistent
150 WRKY18 binding sites defined for 0 h had a more than 1.5 times higher ChIP score or
151 enrichment (ef) score at 2 h (Supplemental Data Set 2). Taking this fact into account, these
152 sites can also be considered to display flg22-dependent enrichment of WRKY18 binding, which
153 is in agreement with the higher WRKY18 protein and RNA levels detected upon flg22
154 stimulation.

155 In certain cases, our automated analysis pipeline failed to detect important target genes, for
156 example due to the applied stringent peak calling, or mis-assignments during the peak
157 annotation step, or for neighboring genes on opposite strands that shared common overlapping
158 promoter regions. To address these issues, we manually inspected the loci of some prominent

159 defense genes not detected by the initial analysis in the IGV for obvious binding peaks. Genes
160 that could be verified as binding targets in this way were added to the corresponding WRKY
161 target lists. Using this strategy, we additionally classified the cysteine-rich receptor-like protein
162 kinase gene *CRK2*, *ISOCHORISMATE SYNTHASE1 (ICS1)*, the glycosyl hydrolase gene
163 *PEN2* and the cytochrome genes *CYP83B1* and *CYP71A13* as targets of WRKY40
164 (Supplemental Figure 1A-E). Moreover, we also rated the leucine-rich repeat serine/threonine
165 protein kinase gene *FLS2*, which is the receptor for flg22, as a likely WRKY target gene,
166 although the automated peak annotation assigned the corresponding binding region to a
167 nearby tRNA gene (Supplemental Figure 1F).

168 As anticipated for transcription factors, more than 97 % of the the binding sites for each of the
169 studied WRKY TFs were located in non-coding DNA regions (Figure 2A), with a clear
170 enrichment in the 1000-bp promoter regions (55 %). About 5 % of the peaks were located in
171 introns, suggesting that some of these introns might also have regulatory capacity. For all three
172 WRKY factors, the binding region peaks were located preferentially within the 400-bp region
173 upstream of the transcription start site (TSS), with the highest frequency of peaks at around
174 position -200 bp (Figure 2B).

175

176 **The W-box is the predominant WRKY factor binding motif**

177 WRKY factors are known to bind to the non-palindromic consensus nucleotide sequence
178 TTGACT/C, termed the W-box. Within the 120 MB Arabidopsis Col0 genome (Tair10), 136,087
179 W-boxes can be identified, with equal numbers on the plus (68,029) and the minus (68,058)
180 DNA strand, which averages roughly to one W-box per 880 bp. The W-box motifs are almost
181 equally distributed among the regions classified as transcription start sites (TSS), transcription
182 termination sites (TTS), exons (CDS), 5'UTRs, 3'UTRs, introns and intergenic regions, again
183 with no preference for the plus or minus strand (Supplemental Figure 2). To detect new or
184 previously known binding motifs in the identified WRKY binding regions, we used the
185 DREME/MEME software suite (Bailey, 2011; Machanick and Bailey, 2011) to perform stringent
186 motif searches within a 500-bp region encompassing the peak summit of each binding region.
187 The corresponding DREME searches for short motifs identified the W-box as the most
188 frequently occurring motif for all three WRKY factors, with one or more W-boxes found in 67 %,

189 72 % and 75 % of the analyzed peak summit regions for WRKY18, WRKY40, and WRKY33,
190 respectively (Figure 3A-C). This indicated that the W-box was the likely binding motif in most of
191 the cases. For all three WRKY factors, the identified W-box motifs were preferentially located
192 close to the binding peak summits, however the probability curves did not display a single
193 sharp central peak, as one would expect for a single binding site per binding region (Figure 3A-
194 C). Consistent with this observation, the number of W-boxes per binding region (which can be
195 larger than the 500 base pairs surrounding the peak summits analyzed in Figure 3A-C) was
196 often higher than one for all tested WRKY factors (Figure 3D), with the number of observed W-
197 boxes being independent of the sizes of the binding regions (Supplemental Figure 3). About 90
198 % of the binding regions contained at least one W-box, and more than 60 % contained two or
199 more. Considering the average size of the binding regions of 730 bp, this clearly indicates an
200 overrepresentation of W-boxes compared to the statistically expected 0.8 W-boxes per region.
201 One prominent example for multiple WRKY factor binding sites within one promoter is the *FLS2*
202 locus, where ten W-boxes within a one kb region with multiple binding peaks for all three
203 WRKY factors were detected (Supplemental Figure 1F). For the identified binding regions a
204 two-fold preference for the W-box sequence TTGACT over the TTGACC motif was observed,
205 mirroring their genomic abundances.

206 Despite the predominance of the W-box motif, binding regions without W-boxes were also
207 observed for all three WRKY factors. This may be indicative of additional W-box sequence-
208 unrelated WRKY factor binding sites or alternatively sites of indirect WRKY binding via other
209 DNA-associated proteins with different DNA binding specificities. When we performed
210 comparable motif searches with the identified binding regions lacking W-boxes, no obvious
211 consensus motifs could be detected.

212

213 **WRKY18 and WRKY40 can bind independently from each other**

214 WRKY18 and WRKY40 were shown previously to form both homo-dimers and hetero-dimers
215 that are capable of binding DNA, and to be redundant in function (Xu et al., 2006; Pandey et
216 al., 2010; Schön et al., 2013). When searching for overlaps between the identified target gene
217 sets of the three WRKY factors, an almost complete overlap of target genes was detected
218 between WRKY18 and WRKY40 after flg22 treatment (87 %), while significantly fewer common

219 targets were observed between WRKY33 and WRKY18 (53 %) or WRKY40 (57 %) (Figure 4,
220 see Suppl. Data Set 3 for sector-specific gene lists).

221 This could suggest that upon flg22 treatment WRKY18 and WRKY40 might have bound as
222 hetero-dimers to the majority of their target sites, while WRKY33 binding occurred more
223 independently. However, when WRKY18-HA or WRKY40-HA were individually expressed in a
224 *wrky18 wrky40* double mutant and ChIP-qPCR was performed on such samples, both factors
225 were still able to bind to tested prominent target loci such as *FLS2*, *BZIP60* and *ERF-1*
226 (Supplemental Figure 4). This observation indicates the ability of WRKY18 and WRKY40 to
227 bind as either homo-dimers or monomers, which could also be the binding modes of WRKY18
228 in the non-induced state. The observed large overlap of WRKY factor target genes could be the
229 result of simultaneous binding to closely spaced W-boxes within the same binding region. It is
230 also possible that seemingly overlapping binding was the result of using whole seedlings for
231 ChIP analyses, as such samples cannot resolve potential selective binding by different WRKY
232 factors within specific tissues (e.g. roots and shoots) or cell types.

233

234 **Binding of WRKY18, WRKY40 and WRKY33 to promoters of genes implicated in MAMP-** 235 **triggered immunity**

236 To investigate the relevance of the identified WRKY target genes for plant defense responses
237 we performed a gene ontology (GO) term enrichment analysis using the GO tool on the TAIR
238 webpage. We found that, compared to the corresponding prevalence in the complete genome,
239 the target gene sets for WRKY18, WRKY40 and WRKY33 were most enriched for genes
240 associated to the cellular component GO term *plasma membrane*, where perception of MAMPs
241 and recognition of pathogens takes place. With respect to molecular functions, genes
242 associated to the GO terms *transferase activity*, *kinase activity*, and *receptor binding or activity*
243 were significantly overrepresented, and these functions are strongly linked to signal
244 transduction to the nucleus upon recognition of pathogens or MAMPs. In agreement with this,
245 the strongest enrichment among the WRKY target genes affected in biological processes was
246 observed for genes connected to the GO terms *response to stress*, *response to abiotic or biotic*
247 *stimulus* and *signal transduction* (Supplemental Figure 5). This result indicates that upon

248 elicitation all three WRKY factors showed a clear preference for binding gene loci involved in
249 the early processes of MTI perception and signaling.

250

251 **Receptor-like kinase (RLKs) genes as targets**

252 Up to 75 receptor (-like) and 64 receptor (-like) kinase genes were identified as targets of
253 WRKY18, WRKY40 and WRKY33 (Supplemental Data Set 4). Among these were genes
254 encoding the prominent plasma membrane-bound MAMP receptors for flagellin (FLS2), chitin
255 (CERK1 and LYM2), and lectin (CES101), as well as genes for the flg22-induced receptor
256 kinase FRK1, the abscisic acid receptor PYL4, the phytosulfokin receptor 1, and four glutamate
257 receptors (GLRs). Further identified WRKY targets were the gene encoding the receptor-
258 associated kinase BIK1 that phosphorylates the ROS-producing NADPH oxidase RBOHD
259 (Macho and Zipfel, 2014) and the *RBOHD* gene itself, as well as genes encoding BIR1, which
260 interacts with BAK1 to negatively regulate different plant resistance pathways (Gao et al.,
261 2009), the G α protein XLG2, which regulates immunity by direct interaction with FLS2 and
262 BIK1 (Liang et al., 2016), AGB1, a heterotrimeric G β protein that acts together with XLG2 and
263 AGG1/AGG2 (G γ proteins) to attenuate proteasome-mediated degradation of BIK1, and
264 PUB12, an E3 ubiquitin ligase involved in the negative regulation of FLS2 by degradation (Lu et
265 al., 2011; Table 2).

266 Interestingly, genes encoding components of damage-associated molecular pattern (DAMP)
267 signaling, including the main receptor PEPR1, the expressed DAMP ligands PROPEP2 and
268 PROPEP3, but not the non-expressed PROPEP1 (Figure 5; Bartels and Boller, 2015), and
269 RLK7, the receptor of PIP1 peptide signaling (Hou et al., 2014), were bound by all three WRKY
270 factors upon flg22 treatment. This suggests that besides WRKY33, which positively regulates
271 expression of *PROPEP2* and *PROPEP3* (Logemann et al., 2013), also the flg22-induced
272 WRKY18 and WRKY40 factors provide a mechanistic and functional link between MTI and
273 DAMP-triggered immunity (DTI). Additionally, several genes encoding receptors of the
274 membrane-bound TIR-NBS-LRR class resistance proteins, usually active during effector-
275 triggered immunity (ETI), were identified as WRKY targets during MTI (Supplemental Data Set
276 1). Taken together, these findings are in full agreement with earlier predictions that numerous

277 *RLK* genes would be targets of WRKY factors, based on the over-representation of W-box
278 elements within their respective promoters (Zipfel et al., 2004).

279 The perception of MAMPs by dedicated receptors triggers various signaling pathways that
280 ultimately give rise to appropriate transcriptional responses within the nucleus. In many cases,
281 such signaling is executed by kinases, transferases and redox-active and reactive proteins
282 through posttranslational modification of proteins within signaling cascades. Protein kinase
283 genes were identified as putative targets of all three WRKY factors, being two-fold
284 overrepresented among the target genes compared to their abundance within the genome.
285 Besides the receptor kinase genes, we additionally identified about 110 kinase genes as
286 WRKY targets, most of which belong to the large families of proteins classified as *kinase-like*
287 *proteins* or *concanavalin A-like lectin kinase proteins*. Furthermore, there were also several
288 kinases from *MAP kinase cascades* and *calcium-dependent protein kinases* identified as
289 WRKY targets, both of which are important signaling components leading to multiple defense
290 responses (Tena et al., 2011; Supplemental Data Set 4). In the case of WRKY40 and
291 WRKY33, all detected binding was dependent on flg22 treatment.

292

293 **WRKY targets connected to hormone pathways**

294 Numerous studies have shown that treatment with pathogens or MAMPs induces hormone
295 signaling and causes the rapid production of plant hormones as well as up-regulation of
296 hormone-response genes (Robert-Seilaniantz et al., 2011; Pieterse et al., 2012). In particular,
297 the ethylene, salicylic acid and jasmonic acid pathways constitute major defense pathways that
298 are highly interconnected, thereby enabling the plant to quickly adapt to changing biotic
299 environments (Tsuda et al., 2009).

300 **Ethylene (ET) pathway**

301 The induction of the ethylene (ET) pathway is one of the earliest events during MTI
302 (Broekgaarden et al., 2015). Two hours after flg22 treatment, we observed induced binding of
303 WRKY18, WRKY40 and WRKY33 to the promoters of key genes in this pathway (Table 3).
304 Among the observed WRKY targets were genes encoding the enzymes of ET biosynthesis
305 ACS2, ACS6 and ACS8, as well as MKK9, which was reported to function upstream of

MPK3/MPK6 in the activation of ACS2 and ACS6 by phosphorylation and binding of WRKY33 (Yoo et al., 2008; Li et al., 2012). Also, the ACC oxidase gene *ACO2*, which catalyzes the final step in the biosynthesis of ET, was a target of the WRKY proteins. Other prominent target genes were *EIN2*, encoding an essential transducer of ET signaling that stabilizes the key ET-dependent gene activator EIN3 (Alonso et al., 1999), and as targets of WRKY18 and WRKY40, the negative regulators of ET signaling *EBF1* and *EBF2* (Gagne et al., 2004). In addition, 34 ET-responsive transcription factor genes (*ERFs*) were found to be targets of the three WRKY factors. Among them were positive regulators like *ERF1*, *ERF-1*, *ERF2*, *ERF5* and *ERF6*, and the negative regulator *ERF4* (Huang et al., 2016). Furthermore, the ERF gene *ORA59* encoding a major integrator of ET and jasmonic acid (JA) signaling (Pré et al., 2008), was identified as an flg22-induced target of WRKY18 and WRKY40. *ORA59* was previously shown also to be a direct target of WRKY33 upon *Botrytis cinerea* infection (Birkenbihl et al., 2012; Liu et al., 2015). Additional targets of all three WRKYs were *MYB51*, which connects ET signaling with indole glucosinolate biosynthesis, and *ABA REPRESSOR1* (*ABR1*), encoding an ERF factor that negatively regulates abscisic acid (ABA)-activated signaling pathways, thereby possibly influencing ET–ABA signal antagonism (Pandey et al., 2005; Clay et al., 2009).

The observed binding of WRKY factors to the promoters of numerous genes encoding components of distinct parts of the pathway, including ET biosynthesis, ET signaling, and transcriptional regulation of the ET response, suggests that these WRKY TFs participate in the regulation of the entire pathway at various levels.

Salicylic acid (SA) pathway

Among the identified WRKY target genes associated with the SA pathway were *ICS1* encoding a key SA biosynthetic enzyme (Garcion et al., 2008), *EDS1* encoding a major component required for host resistance towards various pathogens and an upstream regulator of SA signaling, *SAG101* coding for a key EDS1 interacting protein, *EDS5* encoding a multidrug transporter required for SA accumulation upon pathogen challenge (Serrano et al., 2013), the SA receptor genes *NPR3* and *NPR4* (Fu et al., 2012), *NIMIN1* encoding a negative regulator of NPR1 function (Weigel et al., 2005), *PBS3* encoding an amino acid conjugating GH3 family member regulating SA levels (Okrent et al., 2009), and the resistance gene *SNC1* encoding an immune receptor acting in the EDS1 pathway and requiring SA signaling (Li et al., 2001).

336 Furthermore, several *MYB* and *WRKY* TF genes involved in the regulation of downstream SA
337 responses were identified as targets (Table 4).

338 **Jasmonic acid (JA) pathway**

339 Several genes that encode functions related to JA signaling were also identified as direct
340 targets of the three tested *WRKY* factors. The two JA biosynthetic genes *LIPOXYGENASE3*
341 (*LOX3*) and *ALLENE OXIDE CYCLASE3* (*AOC3*) were targets, as was the amidohydrolase
342 gene *ILL6* that contributes to the turnover of active JA-isoleucine upon wounding (Widemann et
343 al., 2013). Additional targets included *JAZ6* coding for a repressor of JA signaling (Chini et al.,
344 2007), *BOP2* encoding a paralog of *NPR1* essential for pathogen resistance induced by methyl
345 jasmonate (Canet et al., 2012), and the transcription factor genes *ORA59*, *WRKY50* and
346 *WRKY51*. The *WRKY50* and *WRKY51* TFs negatively regulate JA responses following SA
347 treatment or under low 18:1 fatty acid conditions (Gao et al., 2011; Table 5).

348 **Tryptophan-derived secondary metabolite genes as targets**

349 As was the case with the aforementioned signaling- and hormone pathway-associated target
350 genes, the tested *WRKY* factors bound to the promoters of genes encoding diverse functional
351 activities related to the indole secondary metabolites glucosinolates and camalexin, possibly to
352 achieve a more synchronized and robust control of the entire defense system. We detected
353 binding to genes encoding transcriptional regulators as well as biosynthesis enzymes and
354 genes related to the transport of the metabolites. The indolic glucosinolate pathway, emanating
355 from tryptophan, branches at indole-3-acetaldoxime (I3AOx) towards either the production of
356 the phytoalexin camalexin or the generation of indole glucosinolates (Sønderby et al., 2010). In
357 the common part of the pathway, as well as in the downstream branches genes encoding
358 biosynthetic enzymes were detected as flg22-dependent targets of *WRKY18*, *WRKY40* and
359 *WRKY33* (Table 6), including previously reported targets of *WRKY33* upon infection with *B.*
360 *cinerea* (Mao et al., 2011; Birkenbihl et al., 2012; Liu et al., 2015), but also several new gene
361 loci. Among the identified targets were *CYP79B2* encoding the enzyme that participates in
362 converting tryptophan to I3AOx, and *CYP71A12*, *CYP71A13*, *GSTF6*, *GGP1* and *PAD3*,
363 coding for enzymes subsequently converting I3AOx to indole-3-acetonitrile (IAN) and finally to
364 camalexin (Figure 6).

365 Among the genes encoding the indole-glucosinolate core structure-forming enzymes, which
366 convert I3AOx to indol-3-yl-methyl glucosinolate (I3MG), *CYP83B1*, *GSTF9* and *GGP1* were
367 identified as WRKY18 and/or WRKY40 and/or WRKY33 target genes. In addition, the genes
368 coding for *CYP81F2*, and the two indole-glucosinolate methyltransferase genes *IGMT1* and
369 *IGMT2*, which establish secondary modifications leading to 4 (and 1)-methoxy-indol-3-yl-methyl
370 glucosinolate (4MI3MG); Pfalz et al., 2011), were identified as WRKY18, WRKY40 and
371 WRKY33 targets. The genes encoding CYP81F3 and CYP81F4, both also reported to be
372 capable of modifying the indole-ring of I3MG (Pfalz et al., 2011), were not targeted by the
373 WRKY factors. Among the targets of the three tested WRKY TFs were the atypical myrosinase
374 gene *PEN2*, the syntaxin gene *PEN1* and the ABC transporter gene *PEN3*, involved in the
375 production or transport of toxic metabolites derived from 1MI3MG or 4MI3MG (Assaad et al.,
376 2004; Xu et al., 2016). Further WRKY target genes were the flg22-induced TFs *MYB51*, also
377 named *HIGH GLUCOSINOLATE1 (HIG1)*, and *ERF6* that regulate the production of I3AOx or
378 4MI3MG via direct binding to the promoters of the biosynthetic genes *CYP79B2/CYP79B3*
379 (*Frerigmann and Gigolashvili, 2014*), or *CYP81F2*, *IGMT1*, and *IGMT2* (Xu et al., 2016),
380 respectively.

381

382 **Transcription factor genes as targets**

383 A further predominant functional class of WRKY18, WRKY40 and WRKY33 targets upon flg22
384 treatment were transcription factor genes. We found that nearly 10 % of all target genes of the
385 tested WRKY TFs encode transcription factors, which is markedly higher than their relative
386 abundance within the Arabidopsis genome (about 6 %), and an indication that these WRKYs
387 are master regulators of plant immunity. Among the targeted genes, *AP2/ERF* TF genes were
388 highly over-represented (Table 7), which again reflects the importance of ET signaling in early
389 MTI (Broekgaarden et al., 2015).

390 Even more pronounced was the binding of all three WRKY factors to gene loci of their own
391 gene family. WRKY33 binding to the *WRKY33* locus was previously reported (Mao et al.,
392 2011). Here, we found that all three WRKY factors bound to about one third of all WRKY gene
393 promoters, including their own promoters, indicating extensive cross- and auto-regulation within
394 the WRKY TF family upon flg22 elicitation. Of the 32 WRKY genes bound by the three WRKY

395 factors in total, all but three showed significantly up-regulated gene expression (see below and
396 Supplemental Table 1) after 2 h of flg22 treatment (Suppl. Table 1). This preferred binding to
397 the regulatory regions of the WRKY TF gene family was observed earlier for WRKY33 after
398 infection of Arabidopsis with the necrotrophic fungus *Botrytis cinerea* (Liu et al., 2015). In fact,
399 despite distinct modes of elicitation, nearly the same set of WRKY genes reported by Liu et al.
400 (2015) to be targeted by WRKY33 were also found in our study (Supplemental Table 1). These
401 findings suggest that there is a core set of WRKY factors that is activated upon elicitation by
402 different stimuli, and add support to the hypothesis that WRKY factors form a complex sub-
403 regulatory network during the establishment of rapid host defense responses (Eulgem, 2006;
404 Eulgem and Somssich, 2007; Chi et al., 2013; Choura et al., 2015).

405

406 **Transcriptional changes upon flg22 treatment**

407 WRKY18 and WRKY40 have been reported to act as negative regulators of MTI (Xu et al.,
408 2006). To investigate the genome-wide effect of these two TFs in transcriptional changes
409 induced by flg22 treatment, RNA-seq experiments were performed in wildtype plants and
410 *wrky18*, *wrky40*, and *wrky18 wrky40* mutant lines. As for the ChIP-seq experiments, seedlings
411 of each genotype were independently grown for biological replicates in liquid medium and
412 treated with flg22 for 2 h or left untreated. Consistent with previous publications, massive
413 transcriptional changes were observed upon elicitation (Navarro et al., 2004; Zipfel et al., 2004;
414 Zipfel et al., 2006). About 7000 genes in each genotype were altered in their expression upon 2
415 h flg22 treatment compared to untreated seedlings, by at least two-fold (absolute FC ≥ 2) at a
416 false discovery rate (FDR) of less than 0.05 (Supplemental Data Set 5). In all lines about 4000
417 genes were up-regulated and 3000 down-regulated upon flg22 treatment (Table 8, Figure 7A).

418 GO term analysis of the genes with altered expression levels upon flg22 treatment revealed
419 (Supplemental Figure 6): i) Rather small differences in GO term enrichment between the
420 different genotypes, probably due to the high number of differentially expressed genes upon
421 flg22 treatment and the relatively low number of genotype-specific differentially expressed
422 genes (not shown). ii) The terms *unknown cellular components*, *unknown molecular functions*
423 and *unknown biological processes* were clearly under-represented among the flg22-affected
424 genes in WT, reflecting that genes involved in MAMP-triggered immunity have been

extensively investigated. iii) The most obvious differences in GO term enrichment could be observed between up-regulated and down-regulated genes upon flg22 treatment. Thus, the down-regulated genes were strongly enriched for genes associated to the cellular component terms *chloroplast* and *plastid*, which were under-represented among up-regulated genes. Moreover, the up-regulated genes showed a markedly stronger enrichment for genes associated to the molecular function *kinase activity* and the biological processes *response to stress* and *signal transduction*, while the down-regulated genes showed stronger enrichment of genes associated to *cell organization and biogenesis* and *developmental processes*. Together this discrimination in GO terms mirrors the well-described trade-off between plant defense and growth during MTI (Huot et al., 2014; Li et al., 2015).

435

Differentially expressed genes (DEGs) in *wrky18*, *wrky40*, and *wrky18 wrky40*

When we searched for genotype-specific differentially expressed genes (DEGs) in the WRKY mutant lines compared to WT (absolute FC ≥ 2 , FDR < 0.05), we identified in untreated and flg22-treated *wrky18* seedlings only three and six differentially regulated genes, respectively, with one of them being *WRKY18*. In *wrky40* seedlings under the same conditions 14 and 108 DEGs were identified, while in the *wrky18 wrky40* double mutant 112 and 426 genes, respectively, were affected (Figure 7B, Supplemental Data Set 6). The low number of DEGs in the *wrky18* and *wrky40* single mutants compared to the much higher number detected in the double mutant demonstrates the functional redundancy of WRKY18 and WRKY40 at this stage of MTI, with WRKY40 seemingly acting more independent than WRKY18. This redundancy was further confirmed by the high overlap between *wrky40* and *wrky18 wrky40* DEGs, which was 85 % with respect to the *wrky40* gene set, and by the finding that four out of the six *wrky18* DEGs also appeared in the *wrky40* gene set (Figure 7C, see Supplemental Data Set 7 for sector-specific gene lists). Functional redundancy of WRKY18 and WRKY40 was previously demonstrated both in their role as negative regulators of resistance towards the powdery mildew fungus *Golovinomyces orontii* (Pandey et al., 2010), and in positively regulating AvrRPS4 effector-triggered immunity against *Pseudomonas syringae* (Schön et al., 2013). Two hours after flg22 treatment, markedly more DEGs were up-regulated than down-regulated in *wrky40* (88 %) and *wrky18 wrky40* (61 %) compared to WT (Table 9, Figure 7B), indicating that

455 WRKY40, and potentially WRKY18 acting redundantly with WRKY40, were mainly negatively
456 affecting gene expression.

457

458 **Differentially regulated direct target genes (DRTs)**

459 About 55 % of all identified WRKY18, WRKY40 and WRKY33 target genes belonged to the
460 gene set showing altered expression in WT seedlings after flg22 treatment, which is clearly
461 higher than the expected 23 % based on the proportion of genes altered in expression in WT
462 relative to all annotated Arabidopsis genes. About 90 % of these target genes with altered
463 expression levels were up-regulated upon flg22 treatment (Supplemental Figure 7,
464 Supplemental Data Set 8) suggesting that these WRKY factors play a positive regulatory role
465 in reprogramming the transcriptome at this stage of MTI. This apparent discrepancy, that
466 these WRKY factors are negative regulators of most of the differentially expressed genes
467 identified between WT and the respective mutant on the one hand, while their flg22-
468 dependent binding is mainly observed to up-regulated genes in WT plants on the other hand,
469 suggests that they may function to negatively counterbalance the positive effect of other TFs
470 acting at such loci. Candidates for such activators are SARD1, CBP60g and CHE. SARD1
471 and CBP60g belong to the family of calmodulin binding TFs, while CHE is a member of the
472 TCP family. All three TFs have been shown to positively influence defense gene expression
473 and to regulate MTI responses (Truman and Glazebrook, 2012; Zheng et al., 2015). Recent
474 ChIP-seq studies have determined genome-wide binding sites for SARD1 during MTI, and
475 demonstrated substantial redundancy with CBP60g binding (Sun et al., 2015). Comparison
476 between the SARD1 data and our WRKY target gene set revealed a substantial overlap
477 despite differences in the experimental set-ups employed (Supplemental Figure 8, Suppl.
478 Data Set 9). Of the total 392 common targets, 29 are DRTs of WRK18 and WRKY40 and all
479 of these DRTs are up-regulated upon flg22 treatment in the *wrky18 wrky40* double mutant
480 (Suppl. Table 2). One of the common directly regulated target genes, *ICS1*, has been shown
481 to be a direct and positively regulated target not only of SARD1, CBP60g, and CHE (TCP21),
482 but also of other TFs including TCP8 and the NAC TF NTL9 (Wang et al., 2015; Zheng et al.,
483 2015), while in our experiments it was significantly down-regulated by WRKY18 and
484 WRKY40. Similarly, we see a clear negative effect of the WRKY factors on the expression of
485 the receptor-like kinase gene *CRK5*. *CRK5* expression is strongly induced upon flg22-

486 treatment and it is a direct target of WRKY18 and WRKY40, but not WRKY33 (Supplemental
487 Data Set 1; Supplemental Data Set 5). Previous co-transfection assays performed in tobacco
488 leaves revealed that expression of a reporter gene construct driven by the *CRK5* promoter
489 was suppressed by W-box-dependent promoter binding of WRKY18 or WRKY40 (Lu et al.,
490 2016). *ALD1* and *CRK45* are two additional genes that are direct negatively regulated targets
491 of WRKY18 or WRKY40 but are also targets of SARD1. The *ald1* mutant was shown to be
492 compromised in basal resistance and negatively affected in early flg22 responses, while
493 elevated expression of *ALD1* enhanced basal resistance (Song et al., 2004; Cecchini et al.,
494 2015). *CRK45* mutants also showed enhanced basal susceptibility to *Pseudomonas* whereas
495 overexpression lines thereof increased basal resistance (Zhang et al., 2013). Thus, the proper
496 coordinate regulation of defense genes appears rather complex and very likely involves
497 dynamic binding of both positive and negative transcriptional regulators to fine-tune
498 expression and to ensure robust responsiveness to the stimulus.

499

500 To identify directly regulated target genes (DRTs) of WRKY18 and WRKY40, we searched for
501 DEGs between WT and the mutant lines *wrky18*, *wrky40*, and *wrky18 wrky40* that overlapped
502 with the target genes of the respective WRKY factor as identified by ChIP-seq. As the VENN
503 diagram in Figure 8 demonstrates, four loci out of the six DEGs detected in *wrky18* seedlings
504 were bound by WRKY18 after flg22 treatment, including *WRKY18* itself. Fifty-eight (54 %) of
505 the *wrky40* DEG loci were bound by WRKY40, with binding detected only after induction by
506 flg22. In the WRKY40 DRT set *WRKY40* was also found, hinting towards possible feed-back
507 regulation via WRKY18 and WRKY40. Of the DEGs identified in *wrky18 wrky40* seedlings, 122
508 (29 %) and 131 (31 %) gene loci were identified as WRKY18 and WRKY40 direct targets,
509 respectively (see sector specific gene lists in Supplemental Data Set 10 and Supplemental
510 Data Set 11). The overlap between the WRKY18 and WRKY40 DRTs in *wrky18 wrky40* was
511 117 genes, including almost all WRKY18 DRTs (Supplemental Data Set 12), again supporting
512 the notion of a strong functional redundancy of the two WRKY factors and possibly binding to
513 DNA as heterodimers as was previously proposed (Xu et al., 2006). In the same study,
514 WRKY60 was also shown to be capable of forming heterodimers with WRKY18 and WRKY40,
515 and WRKY60 is also a DRT of both. However, its role in MTI remains unclear since expression
516 of this gene is not influenced by flg22, based also on our own RNA-seq data, or by other

517 MAMPs including elf18, chitin, and OGs (oligogalacturonides), according to numerous
518 perturbation studies available at Genvestigator (<https://genevestigator.com/gv/index.jsp>).

519 About 10 % of the WRKY18 or WRKY40 direct target genes showed altered expression upon
520 flg22 treatment in a WRKY18- or WRKY40-dependent manner in the *wrky18 wrky40* double
521 mutant. This relatively poor correlation between TF binding and transcriptional response of
522 target genes has been consistently observed in genome-wide ChIP studies (for possible
523 explanations see Heyendrickx et al. (2014). Conversely, about 30 % of the DEGs between
524 *wrky18 wrky40* and WT identified in this study were bound by WRKY18 or WRKY40. The
525 limited overlap could be due to the dynamics of TF binding, which is often transient and cannot
526 be resolved by analyzing one time point by ChIP-seq as performed here, or to the requirement
527 of additional factors besides TF binding to alter gene expression.

528 Gene ontology analysis of the WRKY18 and WRKY40 DRTs revealed further enrichment of
529 GO terms related to MAMP perception and signaling compared to the overall set of target
530 genes (Supplemental Figure 9). This again is indicative of the two WRKY factors preferentially
531 regulating genes important for early MTI. This further enrichment was observed for the cellular
532 component term *plasma membrane*, the molecular function terms *kinase activity* and
533 *transcription factor activity*, and the biological functions *response to stress*, *response to abiotic*
534 *and biotic stimulus* and *signal transduction*.

535 Among the 117 DRTs common for WRKY18 and WRKY40 were 25 genes encoding kinases,
536 20 of them receptor and receptor-like kinases (including *RK1*, *RK2*, *RLK1*, *CRK20*, *CES101*
537 and *WAKL4*) and together with MKK9 potential perception and signaling components, 16
538 genes for TFs, mainly ERF-type factors important in early MTI and stress-responsive WRKY
539 factors, five genes for VQ motif-containing proteins that can interact with specific WRKY
540 proteins and positively influence their binding to DNA (Jing and Lin, 2015), and seven genes for
541 cytochrome P450 proteins, all of them, together with IGMT1, catalyzing the biosynthesis of
542 secondary metabolites (Bak et al., 2011). Additionally, the three SA pathway-related genes,
543 *ICS1*, *PBS3*, and *NIMIN1*, are DRTs of WRKY18 and WRKY40.

544 As noted above, nearly all of these genes and most of the other DRTs, were flg22-dependently
545 up-regulated in *wrky18 wrky40* compared to WT, indicating that WRKY18 and WRKY40 often
546 fulfill negative regulatory functions in combination with positive regulators at target sites,

547 thereby very likely ensuring proper spatiotemporal transcriptional outputs (Table 10,
548 Supplemental Data Set 7). This negative function in early MAMP-induced responses is in
549 accordance with *wrky18 wrky40* double mutants being less susceptible to the virulent
550 bacterium *Pst* DC3000 than WT (Xu et al., 2006), and with WRKY40 acting together with BZR1
551 in balancing the trade-off between defense and growth (Lozano-Duran et al., 2013). Moreover,
552 it is also consistent with a recent large genome-wide study on ABA-treated Arabidopsis
553 seedlings revealing that highly up-regulated genes are targeted by multiple TFs, and that they
554 act in concert to dynamically modulate transcription and to rapidly restore basal expression
555 levels post stimulation (Song et al., 2016).

556 . In summary, we have defined the genome-wide in vivo binding sites of three Arabidopsis
557 WRKY TFs during early MTI. Our study revealed that the two related WRKY factors WRKY18
558 and WRKY40 targeted nearly the same set of genes during this response, resulting in the
559 altered expression of an almost identical sub-group of genes consistent with these WRKY
560 factors being in part functionally redundant. Moreover, although WRKY33 targets additional
561 unique loci, in many cases it targets the same promoters, or even the same DNA sites as
562 WRKY18 and WRKY40. An additional key finding was that these three WRKY factors target
563 numerous genes encoding key components of both MAMP and DAMP perception and
564 signaling, providing a mechanistic link between these two functionally interconnected basal
565 defense pathways (Albert, 2013; Bartels and Boller, 2015). Finally, our data imply that
566 WRKY18 and WRKY40 are negative-acting regulatory components of numerous flg22-induced
567 early response genes that act together with TF activators to modulate expression in a robust
568 manner. The comprehensive data provide valuable insights that should prove helpful in our
569 endeavor to define the genome-wide transcriptional regulatory network affected by WRKY TFs
570 in the course of plant immunity.

571

572 **Materials and Methods**

573 **Plant material**

574 For all experiments seedlings of the *Arabidopsis thaliana* ecotype Columbia (Col-0) or mutants
575 in the Col-0 background were used. Besides wildtype plants, insertion mutants for *WRKY18*
576 (GABI_328G03), *WRKY40* (SLAT collection of dSpm insertion lines, Shen et al., 2007), and

577 *WRKY33* (GABI_324B11) were used. The double mutant *wrky18 wrky40* was obtained by
578 crossing the corresponding single mutants (Shen et al., 2007). The *ProWRKY33:WRKY33-HA*
579 complementation line in the *wrky33* mutant was described earlier (Birkenbihl et al., 2012). To
580 generate the *ProWRKY18:WRKY18-HA* complementation line, the 5.9 kb genomic fragment
581 (Chromosome 4: nt 15378866-15384809), consisting of the 4.4 kb upstream region up to the
582 next gene and the 1.5 kb intron containing coding region without the stop codon was amplified
583 by PCR, and cloned into the vector pAM-KAN-HA in front of the sequence encoding the HA-
584 epitope tag. For *ProWRKY40:WRKY40-HA*, the 8.7-kb fragment (Chromosome 1: nt
585 30376646-30385353), consisting of a 7.2-kb upstream region and 1.5-kb coding region was
586 used. In both cases, the 3'UTR was replaced by a 35S *CaMV* terminator sequence. All
587 oligonucleotides used in this study are described in Supplemental Table 3. The constructs were
588 transformed via *Agrobacterium* into the respective single mutants.

589 Successfully transformed plants were identified by kanamycin selection. To express the same
590 genomic constructs in the *wrky18 wrky40* double mutant, they were cloned into a pAMP-HYG-
591 HA vector conferring hygromycin resistance to the transformed plants. To confirm functionality
592 of the constructs, transformants were tested for their ability to render resistant *wrky18 wrky40*
593 plants susceptible to the powdery mildew fungus *Golovinomyces orontii* (Pandey et al., 2010).

594 **Plant growth and flg22 treatment**

595 To establish seedling cultures, seeds were surface sterilized with ethanol and subsequently
596 grown in 1x MS medium supplemented with 0.5 % sucrose and 0.1 % claforan. After 12 days in
597 a light chamber at long day conditions (16 h light / 8 h dark) illuminated by daylight-white
598 fluorescence lamps (FL40SS ENW/37; Osram) the seedlings were treated with flg22 by
599 replacing the growth medium with medium containing 1 μ M flg22.

600 **ChIP-seq and ChIP-qPCR experiments**

601 For the ChIP experiments, two independent biological replicates were created at different times
602 with WT and the complementation lines *WRKY18-HA*, *WRKY40-HA*, and *WRKY33-HA*. For each
603 line and treatment, 2 g of whole seedlings were collected from separate cultures 2 h after the
604 medium exchange, either without flg22 (0 h) or with medium containing flg22 (2 h), and processed
605 separately as described previously (Birkenbihl et al., 2012), following the modified protocol of
606 Gendrel et al. (2005). The IPs were performed using a rabbit polyclonal anti-HA antibody (Sigma-

607 Aldrich, St. Louis, MO; catalog number H6908). The precipitated DNA was purified with the Qia
608 quick PCR purification kit (Qiagen, Germany) and processed further for ChIP-seq. To prepare the
609 ChIP-seq libraries, the DNA was first amplified by two rounds of linear DNA amplification (LinDA;
610 Shankaranarayanan et al., 2011) and then libraries were constructed with the NEBNext ChIP-seq
611 Library construction kit (New England Biolabs, Ipswich, MA). The libraries were sequenced at the
612 Max Planck Genome Centre Cologne with an Illumina HiSeq2500, resulting in 7-20 million 100 bp
613 single-end reads per sample.

614

615 **ChIP-seq data analysis**

616 ChIP-seq data processing and analysis was performed as described in Liu et al. (2015) using
617 the TAIR10 *Arabidopsis thaliana* reference genome (<http://www.arabidopsis.org>). The ChIP-
618 seq data created in this study have been deposited at the GEO repository (GSE85922).

619 To identify potential WRKY binding regions ('peak regions'), the QuEST peak calling program
620 (version 2.4; (Valouev et al., 2008) was used as described in Liu et al. (2015) to search for
621 genomic DNA regions enriched in sequencing reads in the WRKY complementation lines
622 compared to the corresponding WT samples. The peak calling was performed separately for
623 the two biological replicates and additionally the mapped reads of both replicates were pooled
624 and peaks were also called for the pooled samples. Peaks were annotated with respect to
625 nearby gene features in TAIR10 using the annotatePeaks.pl function from the Homer suite
626 (Heinz et al., 2010) with default settings. Consistent peaks between the replicates were
627 identified as described in Liu et al. (2015), i.e. peak regions were counted as consistent, if they
628 were found to be overlapping between the both replicates as well as the pooled sample (by at
629 least 50% of the smaller region).

630 To search for conserved binding motifs in the consistent WRKY binding regions, for each
631 consistent peak the 500 bp sequence surrounding the peak maximum was extracted and
632 submitted to the online version of MEME-ChIP (Machanick and Bailey, 2011). MEME-ChIP was
633 run with default settings, but a custom background model derived from the Arabidopsis
634 genome was provided and 'Any number of repetitions' of a motif was allowed. To extract the
635 number/percentage of peak regions that contain a certain motif, the online version of FIMO
636 (Grant et al., 2011) was run with the peak sequences and the motif of interest (either
637 MEME/DREME output or known W-box motif) as input and a p -value threshold of 0.001. To

638 identify all locations of the W-box motif (TTGACT/C) in the complete Arabidopsis genome, the
639 R function 'matchPattern' (Pagès, 2016: *BSgenome: Infrastructure for Biostrings-based*
640 *genome data packages and support for efficient SNP representation*. R package version
641 1.40.1.) was used.

642 **RNA Extraction and Quantitative RT-PCR**

643 For RT-qPCR and the RNA-seq experiments (see below), three independent biological
644 replicates were used: whole seedlings of the indicated genotypes for each treatment were
645 separately grown in three parallel liquid culture sets and processed separately. Total RNA
646 was extracted from 100 mg of untreated or flg22-treated seedlings using the TRI Reagent
647 Solution (Applied Biosystems, AM9738) following the manufacturer's instructions. The RNA
648 was treated with DNase I (Roche) and purified using the RNeasy MiniElute Cleanup Kit
649 (Qiagen, Germany). For RT-qPCR, the RNA was reverse transcribed with an oligo(dT) primer
650 to produce cDNA using the SuperScript First-Strand Synthesis System for Reverse-
651 Transcription PCR following the manufacturer's protocol (Invitrogen). cDNA corresponding to
652 2.5 ng of total RNA was subjected to qPCR with gene-specific primers (Supplemental Table
653 3) using the Brilliant SYBR Green qPCR Core Reagent Kit (Stratagene). The qPCRs were
654 performed on the iQ5 Multicolor Real-Time PCR Detection System (Bio-Rad) with two
655 technical replicates in the same run and the three biological replicates in different runs. The
656 data were analyzed using the DDCT method (Livak and Schmittgen, 2001) and RNA levels are
657 indicated as relative expression compared to the endogenous reference gene At4g26410
658 (Czechowski et al., 2005). Error bars represent the standard deviation of the three biological
659 replicates.

660 **Immunoblot analysis**

661 To analyze the levels of HA-tagged WRKY proteins from seedlings, total proteins were extracted
662 with Laemmli Buffer and equal amounts separated by 8 % SDS-PAGE. The blot was probed with
663 a monoclonal rat antibody against the HA-tag (Roche, Cat. No. 1867423) and developed with a
664 secondary, peroxidase conjugated goat anti rat antibody (Sigma-Aldrich, A9037) using the ECL
665 system according to standard protocols.

666 **RNA-seq experiment**

667 For RNA-seq DNase I-treated and purified RNAs from three biological replicates (as described for
668 RT-qPCR) were used. Libraries for mRNA sequencing were constructed using the TrueSeq RNA
669 Sample preparation Kit (Illumina) and the three biological replicates for each condition were
670 sequenced at the Max Planck Genome Centre Cologne with an Illumina HiSeq2500, resulting in
671 23–44 million 100 bp single end reads per sample. The obtained reads were mapped to the
672 Arabidopsis genome as described in Liu et al. (2015). The RNA-seq data created in this study
673 have been deposited at the GEO repository (GSE85923).

674

675 **RNA-seq data analysis**

676 The mapped RNA-seq reads were transformed into a read count per gene per sample using
677 the htseq-count script (s=reverse, t=exon) in the package HTSeq (Anders et al., 2015). Genes
678 with less than 100 reads in all samples together were discarded, and subsequently the count
679 data of the remaining genes was TMM-normalized and log2-transformed using functions
680 ‘calcNormFactors’ (R package EdgeR; Robinson et al., 2010) and ‘voom’ (R package limma;
681 Law et al., 2014). To be able to analyze differential gene expression both between treated and
682 untreated samples within each genotype and between the different mutants (*wrky18*, *wrky40*,
683 *wrky18 wrky40*) and the WT genotype (Col-0), a linear model with the explanatory variable
684 ‘genotype_treatment’ (i.e., encoding both genotype and treatment information) was fitted for
685 each gene using the function lmFit (R package limma). Subsequently, moderated t-tests were
686 performed over the different contrasts of interest, comparing flg22-treated with untreated
687 samples within each genotype (four contrasts) and comparing each of the mutants with the
688 wildtype within each treatment (six contrasts). In all cases, the resulting p values were adjusted
689 for false discoveries due to multiple hypothesis testing via the Benjamini–Hochberg procedure.
690 For each contrast, we extracted a set of significantly differentially expressed genes between
691 the tested conditions (adj. p value ≤ 0.05 , $|\log_2\text{FC}| \geq 1$).

692 **Gene ontology analysis**

693 For gene ontology analysis, the corresponding tool on the TAIR webpage
694 (<http://www.arabidopsis.org/tools/bulk/go/index.jsp>) was used. The numbers of genes
695 associated to each GO-term in the identified sets of ChIP-seq targets, transcriptionally
696 regulated genes (DEG) and directly regulated target genes (DRT) for each WRKY factor were

697 transformed to relative abundances within each data set and compared to the relative
698 abundance of the respective GO-term in the whole genome. To assess statistical significance
699 of the observed enrichment or under-representation of each GO-term in the different analyzed
700 gene sets, the *p*-values were calculated using a hypergeometric test.

701 **Accession Numbers**

702 The ChIP-seq data and the RNA-seq data created in this study have been deposited at the
703 GEO repository with the accession numbers GSE85922 and GSE85923, respectively. The
704 related GEO Super Series Number is GSE85924.

706 **Supplemental Data**

707 **Supplemental Figures**

708 **Supplemental Figure 1.** IGV images of WRKY18, WRKY40 and WRKY33 binding to the
709 *CRK2*, *ICS1*, *PEN2*, *CYP83B1*, *CYP71A13* and *FLS2* loci.

710 **Supplemental Figure 2.** Distribution of W-box locations in the Arabidopsis genome.

711 **Supplemental Figure 3.** The number of identified W-boxes per binding region is independent
712 of the region size for WRKY18, WRKY40 and WRKY33.

713 **Supplemental Figure 4.** Binding of WRKY18 or WRKY40 to selected target genes in the
714 *wrky18*, *wrky40*, or *wrky18 wrky40* mutant.

715 **Supplemental Figure 5.** GO analysis of WRKY18, WRKY40 and WRKY33 target genes.

716 **Supplemental Figure 6.** GO analysis of genes that exhibit flg22-induced changes of gene
717 expression in WT seedlings.

718 **Supplemental Figure 7.** Up- and down-regulated WRKY target genes upon 2 h flg22
719 treatment.

720 **Supplemental Figure 8:** Target genes common to SARD1 and WRKY18, WRKY40 and
721 WRKY33.

722 **Supplemental Figure 9.** GO analysis of WRKY18 and WRKY40 target genes and their directly
723 regulated targets (DRTs) in *wrky18 wrky40*.

724 **Supplemental Table 1.** WRKY18, WRKY40 and WRKY33 binding to WRKY genes and fold
725 changes of expression of these targets in WT plants upon flg22 treatment.

726 **Supplemental Table 2:** WRKY18 and WRKY40 DRTs in *wrky18 wrky40* that are also bound
727 by SARD1.

728 **Supplemental Table 3.** Primers used for cloning, RT-qPCR and ChIP-qPCR.

729

730 **Supplemental Data Set 1.** Genome-wide binding sites and target genes of WRKY18,
731 WRKY40 and WRKY33 detected after 2 h flg22 treatment.

732 **Supplemental Data Set 2.** Increased enrichment of WRKY18 at target genes defined by
733 clearly higher binding scores at 2 h than at 0 h flg22.

734 **Supplemental Data Set 3.** Overlap between WRKY18, WRKY40 and WRKY33 target gene
735 sets after 2 h flg22 treatment (corresponds to VENN diagram Figure 4).

736 **Supplemental Data Set 4.** WRKY18, WRKY40 and WRKY33 target genes related to the GO-
737 term "kinase activity".

738 **Supplemental Data Set 5.** Flg22-responsive genes in WT plants and *wrky18*, *wrky40*, and
739 *wrky18 wrky40* mutants.

740 **Supplemental Data Set 6.** Differentially expressed genes (DEGs) upon flg22 treatment in
741 *wrky18*, *wrky40*, or *wrky18 wrky40* mutants compared to WT plants.

742 **Supplemental Data Set 7.** Overlap of DEGs in *wrky18*, *wrky40*, or the *wrky18 wrky40* mutant
743 compared to WT plants upon flg22 treatment (corresponds to VENN diagram Figure 7C).

744 **Supplemental Data Set 8.** Up- and down-regulated target and non-target genes in response to
745 flg22 treatment (corresponds to VENN diagram Supplemental Figure 7).

746 **Supplemental Data Set 9:** Target genes common to SARD1 and WRKY18, W40 and W33
747 (corresponds to VENN diagram in Supplemental Figure 8).

748 **Supplemental Data Set 10.** WRKY18 and WRKY40 directly regulated target genes (DRTs;
749 corresponding to VENN diagrams in Figure 8).

750 **Supplemental Data Set 11.** Expression and binding data of WRKY18 and WRKY40 DRTs.

751 **Supplemental Data Set 12.** Directly regulated targets (DRTs) common to WRKY18 and
752 WRKY40.

753

754 **Acknowledgements**

755 This work was supported by the Deutsche Forschungsgemeinschaft (DFG) by a grant in the
756 frame work of SFB670 Cell Autonomous Immunity (IES and BK).

757

758 **Author Contributions**

759 RPB, conception and design, conducted experiments, acquisition of data, analysis and
760 interpretation of data, drafting and revising the manuscript; BK, analysis and interpretation of
761 data, drafting and revising the manuscript; IES, conception and design, analysis and
762 interpretation of data, drafting and revising the manuscript.

763

764 **References**

765 **Albert, M.** (2013). Peptides as triggers of plant defence. *J. Exp. Bot.* **64**, 5269-5279.

766 **Alonso, J.M., Hirayama, T., Roman, G., Nourizadeh, S., and Ecker, J.R.** (1999). EIN2, a
767 bifunctional transducer of ethylene and stress responses in *Arabidopsis*. *Science* **284**,
768 2148-2152.

769 **Anders, S., Pyl, P.T., and Huber, W.** (2015). HTSeq—a Python framework to work with high-
770 throughput sequencing data. *Bioinformatics* **31**, 166-169.

771 **Assaad, F.F., Qiu, J.-L., Youngs, H., Ehrhardt, D., Zimmerli, L., Kalde, M., Wanner, G.,**
772 **Peck, S.C., Edwards, H., Ramonell, K., Somerville, C.R., and Thordal-Christensen,**
773 **H.** (2004). The PEN1 syntaxin defines a novel cellular compartment upon fungal attack
774 and is required for the timely assembly of papillae. *Mol. Biol. Cell* **15**, 5118-5129.

775 **Bailey, T.L.** (2011). DREME: motif discovery in transcription factor ChIP-seq data.
776 *Bioinformatics* **27**, 1653-1659.

777 **Bailey, T.L., and Machanick, P.** (2012). Inferring direct DNA binding from ChIP-seq. *Nucleic*
778 *Acids Res.* **40**, e128.

779 **Bak, S., Beisson, F., Bishop, G., Hamberger, B., Höfer, R., Paquette, S., and Werck-**
780 **Reichhart, D.** (2011). Cytochromes P450. *The Arabidopsis Book*, e0144.

781 **Bartels, S., and Boller, T.** (2015). Quo vadis, Pep? Plant elicitor peptides at the crossroads of
782 immunity, stress, and development. *J. Exp. Bot.* **66**, 5183-5193.

783 **Birkenbihl, R.P., Diezel, C., and Somssich, I.E.** (2012). Arabidopsis WRKY33 is a key
784 transcriptional regulator of hormone and metabolic responses towards *Botrytis cinerea*
785 infection. *Plant Physiol.* **159**, 266-285.

786 **Broekgaarden, C., Caarls, L., Vos, I.A., Pieterse, C.M.J., and Van Wees, S.C.M.** (2015).
787 Ethylene: Traffic controller on hormonal crossroads to defense. *Plant Physiol.* **169**,
788 2371-2379.

789 **Canet, J.V., Dobón, A., Fajmonová, J., and Tornero, P.** (2012). The BLADE-ON-PETIOLE
790 genes of Arabidopsis are essential for resistance induced by methyl jasmonate. *BMC*
791 *Plant Biol* **12**, 199.

792 **Cecchini, N.M., Jung, H.W., Engle, N.L., Tschaplinski, T.J., and Greenberg, J.T.** (2014).
793 ALD1 regulates basal immune components and early inducible defense responses in
794 *Arabidopsis*. *Mol. Plant-Microbe Interact.* **28**, 455-466.

795 **Chi, Y., Yang, Y., Zhou, Y., Zhou, J., Fan, B., Yu, J.-Q., and Chen, Z.** (2013). Protein-protein
796 interactions in the regulation of WRKY transcription factors. *Mol. Plant* **6**, 287-300.

797 **Chini, A., Fonseca, S., Fernandez, G., Adie, B., Chico, J.M., Lorenzo, O., Garcia-Casado,**
798 **G., Lopez-Vidriero, I., Lozano, F.M., Ponce, M.R., Micol, J.L., and Solano, R.** (2007).
799 The JAZ family of repressors is the missing link in jasmonate signalling. *Nature* **448**,
800 666-671.

801 **Choura, M., Rebai, A., and Masmoudi, K.** (2015). Unraveling the WRKY transcription factors
802 network in *Arabidopsis thaliana* by integrative approach. *Network Biol.* **5**, 55-61.

803 **Clay, N.K., Adio, A.M., Denoux, C., Jander, G., and Ausubel, F.M.** (2009). Glucosinolate
804 metabolites required for an *Arabidopsis* innate immune response. *Science* **323**, 95-101.

805 **Czechowski, T., Stitt, M., Altmann, T., Udvardi, M.K., and Scheible, W.-R.** (2005). Genome-
806 wide identification and testing of superior reference genes for transcript normalization in
807 *Arabidopsis*. *Plant Physiol.* **139**, 5-17.

808 **Eulgem, T.** (2006). Dissecting the WRKY web of plant defense regulators. *PLoS Pathog.* **2**,
809 e126.

810 **Eulgem, T., and Somssich, I.E.** (2007). Networks of WRKY transcription factors in defense
811 signaling. *Curr. Opin. Plant Biol.* **10**, 366-371.

812 **Felix, G., Duran, J.D., Volko, S., and Boller, T.** (1999). Plants have a sensitive perception
813 system for the most conserved domain of bacterial flagellin. *Plant J.* **18**, 265-276.

814 **Frerigmann, H., and Gigolashvili, T.** (2014). MYB34, MYB51, and MYB122 distinctly regulate
815 indolic glucosinolate biosynthesis in *Arabidopsis thaliana*. *Mol. Plant* **7**, 814-828.

816 **Fu, Z.Q., Yan, S., Saleh, A., Wang, W., Ruble, J., Oka, N., Mohan, R., Spoel, S.H., Tada, Y.,
817 Zheng, N., and Dong, X.** (2012). NPR3 and NPR4 are receptors for the immune signal
818 salicylic acid in plants. *Nature* **486**, 228-232.

819 **Gagne, J.M., Smalle, J., Gingerich, D.J., Walker, J.M., Yoo, S.-D., Yanagisawa, S., and
820 Vierstra, R.D.** (2004). Arabidopsis EIN3-binding F-box 1 and 2 form ubiquitin-protein
821 ligases that repress ethylene action and promote growth by directing EIN3 degradation.
822 *Proc. Natl. Acad. Sci. USA* **101**, 6803-6808.

823 **Gao, M., Wang, X., Wang, D., Xu, F., Ding, X., Zhang, Z., Bi, D., Cheng, Y.T., Chen, S., Li,
824 X., and Zhang, Y.** (2009). Regulation of cell death and innate immunity by two receptor-
825 like kinases in *Arabidopsis*. *Cell Host Microbe* **6**, 34-44.

826 **Gao, Q.-M., Venugopal, S., Navarre, D., and Kachroo, A.** (2011). Low oleic acid-derived
827 repression of jasmonic acid-inducible defense responses requires the WRKY50 and
828 WRKY51 proteins. *Plant Physiol.* **155**, 464-476.

829 **Garcion, C., Lohmann, A., Lamodiére, E., Catinot, J., Buchala, A., Doermann, P., and
830 Metraux, J.-P.** (2008). Characterization and biological function of the *ISOCHORISMATE*
831 *SYNTHASE2* gene of *Arabidopsis*. *Plant Physiol.* **147**, 1279-1287.

832 **Gendrel, A.-V., Lippman, Z., Martienssen, R., and Colot, V.** (2005). Profiling histone
833 modification patterns in plants using genomic tiling microarrays. *Nat. Meth.* **2**, 213-218.

834 **Grant, C.E., Bailey, T.L., and Noble, W.S.** (2011). FIMO: scanning for occurrences of a given
835 motif. *Bioinformatics* **27**.

836 **Heinz, S., Benner, C., Spann, N., Bertolino, E., Lin, Y.C., Laslo, P., Cheng, J.X., Murre, C.,**
837 **Singh, H., and Glass, C.K.** (2010). Simple combinations of lineage-determining
838 transcription factors prime *cis*-regulatory elements required for macrophage and B cell
839 identities. *Mol. Cell* **38**, 576-589.

840 **Heyndrickx, K.S., de Velde, J.V., Wang, C., Weigel, D., and Vandepoele, K.** (2014). A
841 functional and evolutionary perspective on transcription factor binding in *Arabidopsis*
842 *thaliana*. *Plant Cell* **26**, 3894-3910.

843 **Hou, S., Wang, X., Chen, D., Yang, X., Wang, M., Turrà, D., Di Pietro, A., and Zhang, W.**
844 (2014). The secreted peptide PIP1 amplifies immunity through receptor-like kinase 7.
845 *PLoS Pathog.* **10**, e1004331.

846 **Huang, P.-Y., Catinot, J., and Zimmerli, L.** (2016). Ethylene response factors in *Arabidopsis*
847 immunity. *J. Exp. Bot.* **67**, 1231-1241.

848 **Huot, B., Yao, J., Montgomery, B.L., and He, S.Y.** (2014). Growth-defense tradeoffs in
849 plants: a balancing act to optimize fitness. *Mol. Plant* **7**, 1267-1287.

850 **Jing, Y., and Lin, R.** (2015). The VQ motif-containing protein family of plant-specific
851 transcriptional regulators. *Plant Physiol.* **169**, 371-378.

852 **Kadota, Y., Sklenar, J., Derbyshire, P., Stransfeld, L., Asai, S., Ntoukakis, V., Jones,**
853 **Jonathan D., Shirasu, K., Menke, F., Jones, A., and Zipfel, C.** (2014). Direct
854 Regulation of the NADPH Oxidase RBOHD by the PRR-Associated Kinase BIK1 during
855 Plant Immunity. *Mol. Cell* **54**, 43-55.

856 **Law, C., Chen, Y., Shi, W., and Smyth, G.** (2014). voom: precision weights unlock linear
857 model analysis tools for RNA-seq read counts. *Genome Biol.* **15**, R29.

858 **Li, B., Meng, X., Shan, L., and He, P.** (2016). Transcriptional regulation of pattern-triggered
859 immunity in plants. *Cell Host Microbe* **19**, 641-650.

860 **Li, G., Meng, X., Wang, R., Mao, G., Han, L., Liu, Y., and Zhang, S.** (2012). Dual-level
861 regulation of ACC synthase activity by MPK3/MPK6 cascade and its downstream WRKY
862 transcription factor during ethylene induction in *Arabidopsis*. *PLoS Genet.* **8**, e1002767.

863 **Li, R., Zhang, J., Li, J., Zhou, G., Wang, Q., Bian, W., Erb, M., and Lou, Y.** (2015).
864 Prioritizing plant defence over growth through WRKY regulation facilitates infestation by
865 non-target herbivores. *eLIFE* **4**, e04805.

866 **Li, X., Clarke, J.D., Zhang, Y., and Dong, X.** (2001). Activation of an EDS1-mediated *R*-gene
867 pathway in the *snc1* mutant leads to constitutive, NPR1-independent pathogen
868 resistance. *Mol. Plant-Microbe Interact.* **14**, 1131-1139.

869 **Liang, X., Ding, P., Lian, K., Wang, J., Ma, M., Li, L., Li, L., Li, M., Zhang, X., Chen, S.,**
870 **Zhang, Y., and Zhou, J.-M.** (2016). Arabidopsis heterotrimeric G proteins regulate
871 immunity by directly coupling to the FLS2 receptor. *eLife* **5**, e13568.

872 **Liu, S., Kracher, B., Ziegler, J., Birkenbihl, R.P., and Somssich, I.E.** (2015). Negative
873 regulation of ABA signaling by WRKY33 is critical for *Arabidopsis* immunity towards
874 *Botrytis cinerea* 2100. *eLIFE* **4**, e07295.

875 **Livak, K.J., and Schmittgen, T.D.** (2001). Analysis of relative gene expression data using real-
876 time quantitative PCR and the 2(-Delta Delta C(T)) Method. *Methods* **25**, 402-408.

877

878 **Logemann, E., Birkenbihl, R.P., Rawat, V., Schneeberger, K., Schmelzer, E., and**
879 **Somssich, I.E.** (2013). Functional dissection of the PROPEP2 and PROPEP3
880 promoters reveals the importance of WRKY factors in mediating microbe-associated
881 molecular pattern-induced expression. *New Phytol.* **198**, 1165-1177.

882 **Lozano-Durán, R., Macho, A.P., Boutrot, F., Segonzac, C., Somssich, I.E., and Zipfel, C.**
883 (2013). The transcriptional regulator BZR1 mediates trade-off between plant innate
884 immunity and growth. *eLife* **2**, e00983.

885 **Lu, D., Lin, W., Gao, X., Wu, S., Cheng, C., Avila, J., Heese, A., Devarenne, T.P., He, P.,**
886 **and Shan, L.** (2011). Direct ubiquitination of pattern recognition receptor FLS2
887 attenuates plant innate immunity. *Science* **332**, 1439-1442.

888 **Lu, K., Liang, S., Wu, Z., Bi, C., Yu, Y.-T., Wang, X.-F., and Zhang, D.-P.** (2016).
889 Overexpression of an Arabidopsis cysteine-rich receptor-like protein kinase, *CRK5*,
890 enhances abscisic acid sensitivity and confers drought tolerance. *J. Exp. Bot.* **67**, 5009-
891 5027.

892 **Machanick, P., and Bailey, T.** (2011). MEME-ChIP: motif analysis of large DNA datasets.
893 *Bioinformatics* **27**, 1696 - 1697.

894 **Macho, A.P., and Zipfel, C.** (2014). Plant PRRs and the activation of innate immune signaling.
895 *Mol. Cell* **54**.

896 **Mao, G., Meng, X., Liu, Y., Zheng, Z., Chen, Z., and Zhang, S.** (2011). Phosphorylation of a
 897 WRKY Transcription Factor by Two Pathogen-Responsive MAPKs Drives Phytoalexin
 898 Biosynthesis in *Arabidopsis*. *Plant Cell* **23**, 1639-1653.

899 **Monaghan, J., and Zipfel, C.** (2012). Plant pattern recognition receptor complexes at the
 900 plasma membrane. *Curr. Opin. Plant Biol.* **15**, 1-9.

901 **Møldrup, M.E., Salomonsen, B., Geu-Flores, F., Olsen, C.E., and Halkier, B.A.** (2013). De
 902 novo genetic engineering of the camalexin biosynthetic pathway. *J. Biotechnol.* **167**,
 903 296-301.

904 **Navarro, L., Zipfel, C., Rowland, O., Keller, I., Robatzek, S., Boller, T., and Jones, J.D.G.**
 905 (2004). The transcriptional innate immune response to flg22. Interplay and overlap with
 906 *avr* gene-dependent defense responses and bacterial pathogenesis. *Plant Physiol.* **135**,
 907 1113-1128.

908 **Newman, M.-A., Sundelin, T., Nielsen, J.T., and Erbs, G.** (2013). MAMP (Microbe-
 909 Associated Molecular Pattern) triggered immunity in Plants. *Front. Plant Sci.* **4**, 139.

910 **Okrent, R.A., Brooks, M.D., and Wildermuth, M.C.** (2009). *Arabidopsis* GH3.12 (PBS3)
 911 conjugates amino acids to 4-substituted benzoates and is inhibited by salicylate. *J. Biol.*
 912 *Chem.* **284**, 9742-9754.

913 **Pandey, G.K., Grant, J.J., Cheong, Y.H., Kim, B.G., Li, L., and Luan, S.** (2005). ABR1, an
 914 APETALA2-domain transcription factor that functions as a repressor of ABA response in
 915 *Arabidopsis*. *Plant Physiol.* **139**, 1185-1193.

916 **Pandey, S.P., Roccaro, M., Schön, M., Logemann, E., and Somssich, I.E.** (2010).
 917 Transcriptional reprogramming regulated by WRKY18 and WRKY40 facilitates powdery
 918 mildew infection of *Arabidopsis*. *Plant J.* **64**, 912-923.

919 **Pfalz, M., Mikkelsen, M.D., Bednarek, P., Olsen, C.E., Halkier, B.A., and Kroymann, J.**
 920 (2011). Metabolic engineering in *Nicotiana benthamiana* reveals key enzyme functions
 921 in *Arabidopsis* indole glucosinolate modification. *Plant Cell* **23**, 716-729.

922 **Pieterse, C.M.J., Van der Does, D., Zamioudis, C., Leon-Reyes, A., and Van Wees, S.C.M.**
 923 (2012). Hormonal modulation of plant immunity. *Annu. Rev. Cell. Dev. Biol.* **28**, 489-521.

924 **Pré, M., Atallah, M., Champion, A., De Vos, M., Pieterse, C.M.J., and Memelink, J.** (2008).
 925 The AP2/ERF domain transcription factor ORA59 integrates jasmonic acid and ethylene
 926 signals in plant defense. *Plant Physiol.* **147**, 1347-1357.

927 **Qiu, J.-L., Fiil, B.-K., Petersen, K., Nielsen, H.B., Botanga, C.J., Thorgrimsen, S., Palma,**
928 **K., Suarez-Rodriguez, M.C., Sandbech-Clausen, S., Lichota, J., Brodersen, P.,**
929 **Grasser, K.D., Mattsson, O., Glazebrook, J., Mundy, J., and Petersen, M. (2008).**
930 *Arabidopsis* MAP kinase 4 regulates gene expression through transcription factor
931 release in the nucleus. *EMBO J.* **27**, 2214-2221.

932 **Robert-Seilaniantz, A., Grant, M., and Jones, J.D.G. (2011).** Hormone crosstalk in plant
933 disease and defense: More than just JASMONATE-SALICYLATE antagonism. *Annu.*
934 *Rev. Phytopathol.* **49**, 317-343.

935 **Robinson, M.D., McCarthy, D.J., and Smyth, G.K. (2010).** edgeR: a Bioconductor package
936 for differential expression analysis of digital gene expression data. *Bioinformatics* **26**,
937 139-140.

938 **Rushton, P.J., Somssich, I.E., Ringler, P., and Shen, Q.J. (2010).** WRKY transcription
939 factors. *Trends Plant Sci.* **15**, 247-258.

940 **Schön, M., Töller, A., Diezel, C., Roth, C., Westphal, L., Wiermer, M., and Somssich, I.E.**
941 **(2013).** Analyses of wrky18 wrky40 plants reveal critical roles of SA/EDS1 signaling and
942 indole-glucosinolate biosynthesis for *Golovinomyces orontii* resistance and a loss-of
943 resistance towards *Pseudomonas syringae* pv. *tomato* AvrRPS4. *Mol. Plant-Microbe*
944 *Interact.* **26**, 758-767.

945 **Schweizer, F., Bodenhausen, N., Lassueur, S., Masclaux, F.G., and Reymond, P. (2013).**
946 Differential contribution of transcription factors to *Arabidopsis thaliana* defence against
947 *Spodoptera littoralis*. *Front. Plant Sci.* **4**, 13.

948 **Schwessinger, B., and Ronald, P.C. (2012).** Plant innate immunity: perception of conserved
949 microbial signatures. *Annu. Rev. Plant Biol.* **63**, 451-482.

950 **Serrano, M., Wang, B., Aryal, B., Garcion, C., Abou-Mansour, E., Heck, S., Geisler, M.,**
951 **Mauch, F., Nawrath, C., and Métraux, J.-P. (2013).** Export of salicylic acid from the
952 chloroplast requires the multidrug and toxin extrusion-like transporter EDS5. *Plant*
953 *Physiol.* **162**, 1815-1821.

954 **Shankaranarayanan, P., Mendoza-Parra, M.-A., Walia, M., Wang, L., Li, N., Trindade, L.M.,**
955 **and Gronemeyer, H. (2011).** Single-tube linear DNA amplification (LinDA) for robust
956 ChIP-seq. *Nat. Meth.* **8**, 565-567.

957 **Shen, Q.-H., Saijo, Y., Mauch, S., Biskup, C., Bieri, S., Keller, B., Seki, H., Ulker, B.,**
958 **Somssich, I.E., and Schulze-Lefert, P. (2007).** Nuclear activity of MLA immune

959 receptors links isolate-specific and basal disease-resistance responses. *Science* **315**,
 960 1098-1103.

961 **Sønderby, I.E., Geu-Flores, F., and Halkier, B.A.** (2010). Biosynthesis of glucosinolates -
 962 gene discovery and beyond. *Trends Plant Sci.* **15**, 283-290.

963 **Song, J.T., Lu, H., McDowell, J.M., and Greenberg, J.T.** (2004). A key role for ALD1 in
 964 activation of local and systemic defenses in *Arabidopsis*. *Plant J.* **40**, 200-212.

965 **Song, L., Huang, S.-s.C., Wise, A., Castanon, R., Nery, J.R., Chen, H., Watanabe, M.,**
 966 **Thomas, J., Bar-Joseph, Z., and Ecker, J.R.** (2016). A transcription factor hierarchy
 967 defines an environmental stress response network. *Science* **354**, 598.

968 **Sun, T., Zhang, Y., Li, Y., Zhang, Q., Ding, Y., and Zhang, Y.** (2015). ChIP-seq reveals broad
 969 roles of SARD1 and CBP60g in regulating plant immunity. *Nat. Commun.* **6**, 10159.

970 **Sun, Y., Li, L., Macho, A.P., Han, Z., Hu, Z., Zipfel, C., Zhou, J.-m., and Chai, J.** (2013).
 971 Structural basis for flg22-induced activation of the *Arabidopsis* FLS2-BAK1 immune
 972 complex. *Science* **342**, 224-628.

973 **Tena, G., Boudsocq, M., and Sheen, J.** (2011). Protein kinase signaling networks in plant
 974 innate immunity. *Curr. Opin. Plant Biol.* **14**, 519-529.

975 **Thorvaldsdóttir, H., Robinson, J.T., and Mesirov, J.P.** (2013). Integrative Genomics Viewer
 976 (IGV): high-performance genomics data visualization and exploration. *Briefings in*
 977 *Bioinformatics* **14**, 178-192.

978 **Truman, W., and Glazebrook, J.** (2012). Co-expression analysis identifies putative targets for
 979 CBP60g and SARD1 regulation. *BMC Plant Biol* **12**, 216.

980 **Tsuda, K., and Somssich, I.E.** (2015). Transcriptional networks in plant immunity. *New Phytol.*
 981 **206**, 932-947.

982 **Tsuda, K., Sato, M., Stoddard, T., Glazebrook, J., and Katagiri, F.** (2009). Network
 983 properties of robust immunity in plants. *PLoS Genet.* **5**, e1000772.

984 **Valouev, A., Johnson, D.S., Sundquist, A., Medina, C., Anton, E., Batzoglou, S., Myers,**
 985 **R.M., and Sidow, A.** (2008). Genome-wide analysis of transcription factor binding sites
 986 based on ChIP-Seq data. *Nat. Meth.* **5**, 829-834.

987 **Vidhyasekaran, P.** (2014). PAMP signaling in plant innate immunity. In *PAMP Signals in Plant*
 988 *Innate Immunity - Signal Perception and Transduction* (Springer), pp. 17-161.

989 **Wan, J., Zhang, X.-C., Neece, D., Ramonell, K.M., Clough, S., Kim, S.-y., Stacey, M.G., and**
990 **Stacey, G. (2008).** A LysM receptor-like kinase plays a critical role in chitin signaling
991 and fungal resistance in *Arabidopsis*. *Plant Cell* **20**, 471-481.

992 **Wang, X., Gao, J., Zhu, Z., Dong, X., Wang, X., Ren, G., Zhou, X., and Kuai, B. (2015).** TCP
993 transcription factors are critical for the coordinated regulation of *ISOCHORISMATE*
994 *SYNTHASE 1* expression in *Arabidopsis thaliana*. *Plant J.* **82**, 151-162.

995 **Weigel, R.R., Pfitzner, U.M., and Gatz, C. (2005).** Interaction of NIMIN1 with NPR1 modulates
996 PR gene expression in *Arabidopsis*. *Plant Cell* **17**, 1279-1291.

997 **Widemann, E., Miesch, L., Lugan, R., Holder, E., Heinrich, C., Aubert, Y., Miesch, M.,**
998 **Pinot, F., and Heitz, T. (2013).** The amidohydrolases IAR3 and ILL6 contribute to
999 jasmonoyl-isoleucine hormone turnover and generate 12-hydroxyjasmonic acid upon
1000 wounding in *Arabidopsis* leaves. *J. Biol. Chem.* **288**, 31701-31714.

1001 **Xu, J., Meng, J., Meng, X., Zhao, Y., Liu, J., Sun, T., Liu, Y., Wang, Q., and Zhang, S.**
1002 **(2016).** Pathogen-responsive MPK3 and MPK6 reprogram the biosynthesis of indole
1003 glucosinolates and their derivatives in *Arabidopsis* immunity. *Plant Cell* **28**, 1144-1162.

1004 **Xu, X., Chen, C., Fan, B., and Chen, Z. (2006).** Physical and functional interactions between
1005 pathogen-induced *Arabidopsis* WRKY18, WRKY40, and WRKY60 transcription factors.
1006 *Plant Cell* **18**, 1310-1326.

1007 **Yoo, S.-D., Cho, Y.-H., Tena, G., Xiong, Y., and Sheen, J. (2008).** Dual control of nuclear
1008 EIN3 by bifurcate MAPK cascades in C2H4 signalling. *Nature* **451**, 789-795.

1009 **Zhang, X., Han, X., Shi, R., Yang, G., Qi, L., Wang, R., and Li, G. (2013).** *Arabidopsis*
1010 cysteine-rich receptor-like kinase 45 positively regulates disease resistance to
1011 *Pseudomonas syringae*. *Plant Physiol. Biochem.* **73**, 383-391.

1012 **Zheng, X.-y., Zhou, M., Yoo, H., Pruneda-Paz, J.L., Spivey, N.W., Kay, S.A., and Dong, X.**
1013 **(2015).** Spatial and temporal regulation of biosynthesis of the plant immune signal
1014 salicylic acid. *Proc. Natl. Acad. Sci. USA* **112**, 9166-9173.

1015 **Zheng, Z., Qamar, S.A., Chen, Z., and Mengiste, T. (2006).** *Arabidopsis* WRKY33
1016 transcription factor is required for resistance to necrotrophic fungal pathogens. *Plant J.*
1017 **48**, 592-605.

1018 **Zipfel, C., Robatzek, S., Navarro, L., Oakeley, E.J., Jones, J.D.G., Felix, G., and Boller, T.**
1019 **(2004).** Bacterial disease resistance in *Arabidopsis* through flagellin perception. *Nature*
1020 **428**, 764-767.

1021 **Zipfel, C., Kunze, G., Chinchilla, D., Caniard, A., Jones, J.D.G., Boller, T., and Felix, G.**
1022 (2006). Perception of the bacterial PAMP EF-Tu by the receptor EFR restricts
1023 *Agrobacterium*-mediated transformation. *Cell* **125**, 749-760.

1024

1025 **Figure Legends**

1026 **Figure 1.** Induction of *WRKY18*, *WRKY40* and *WRKY33* by flg22 treatment. A. RT-qPCR
1027 analysis of flg22-induced RNA levels. Total RNA was isolated from seedlings treated for 0, 1, 2
1028 and 4 h with flg22 and analyzed by qPCR using gene-specific primers. Shown are the mean
1029 and standard deviation (error bars) calculated from three biological replicates. B. Immunoblot
1030 analysis of flg22-induced protein levels. Protein extracts from seedlings of the HA-tagged
1031 complementation lines were treated for indicated times with flg22 and subsequently analyzed
1032 by immunoblot using an anti-HA antibody. Ponceau S staining served as loading control.

1033 **Figure 2.** Distribution of flg22-induced *WRKY18*, *WRKY40* and *WRKY33* binding regions in the
1034 *Arabidopsis* genome. A. Prevalence of WRKY binding regions in different genomic categories.
1035 Promoters are defined as the 1000-bp region upstream of the transcription start site (TSS).
1036 Transcription termination site (TTS) refers to the 1000-bp region downstream of the 3'UTR, and
1037 genome regions located in between a TTS and the promoter of the next gene are regarded as
1038 intergenic. B. Distance of WRKY binding region peaks to the transcription start site. The
1039 number of binding region peaks for each 50-bp region relative to the TSS is indicated.

1040 **Figure 3.** The W-box is the predominant motif within WRKY binding regions. A, B, C. Motif
1041 position probability graphs for *WRKY18* (A), *WRKY40* (B) and *WRKY33* (C) established by
1042 CentriMo motif search (Bailey and Machanick, 2012). Indicated is the most frequent motif, its
1043 rate of occurrence, and the probability of this motif occurring at a given position relative to the
1044 binding peak summit (0) in the 500-bp binding regions. The included p-value describes the
1045 significance for central enrichment. D. Distribution of W-box abundances in *WRKY18*, *WRKY40*
1046 and *WRKY33* binding regions.

1047 **Figure 4.** Overlap of *WRKY18*, *WRKY40* and *WRKY33* target gene sets after 2 h flg22
1048 treatment. Indicated are the number of target genes in each section, and the fraction of
1049 overlapping genes between each pair of WRKY target gene sets with respect to the smaller set.

1050 **Figure 5.** WRKY18, WRKY40 and WRKY33 binding to the *PEPR1*, *PROPEP2* and *PROPEP3*
1051 loci. A. Integrative Genome Viewer (IGV) images of the *PEPR1* (A) and *PROPEP1-3* loci (B).
1052 Binding of WRKYs is visualized by read coverage histograms indicating sequencing read
1053 accumulation before (0 h) or after flg22 treatment (2 h). WT samples served as negative control.
1054 The three lower tracks show the corresponding gene structures, position of W-boxes and the
1055 direction of transcription (arrows).

1056 **Figure 6.** WRKY18, WRKY40 and WRKY33 bind to genes involved in biosynthesis and
1057 transport of secondary metabolites camalexin and indole-glucosinolates (biosynthetic pathways
1058 adapted from Sonderby et al., 2010; Pfalz et al., 2011; Morldrup et al., 2013). Identified
1059 WRKY18, WRKY40 or WRKY33 target genes are indicated in yellow. TFs are underlined.

1060 **Figure 7.** Differentially expressed genes in *wrky18*, *wrky40*, and *wrky18 wrky40* plants. A.
1061 Number of significantly ($FC \geq 2$, $FDR < 0.05$) up- or down-regulated genes at 2 h flg22 treatment
1062 compared to 0 h in the indicated genotype. B. Number of up- and down-regulated, differentially
1063 expressed genes (DEGs) ($FDR < 0.05$, $FC \geq 2$) in the respective mutant lines compared to WT at
1064 0, 1, or 2 h post flg22 treatment. C. Overlap of the identified sets of DEGs in the respective
1065 mutant lines relative to WT at 2 h post flg22 treatment. Indicated are the number of DEGs in each
1066 section.

1067 **Figure 8.** Directly regulated target genes (DRTs) of WRKY18 and WRKY40. DRTs were identified
1068 by the overlaps of the WRKY18 and WRKY40 target gene sets with the sets of differentially
1069 expressed genes (DEGs) compared to WT in *wrky18*, *wrky40* and *wrky18 wrky40* mutants at 2 h
1070 post flg22 treatment. Indicated are the number of target genes, DEGs and DRTs in the respective
1071 sections, and the fraction DEGs identified as DRTs in each comparison.

1072

1073 **Tables**

1074

1075 **Table 1:** Flg22-induced WRKY18, WRKY40 and WRKY33 binding sites and target genes

1076

TFs	Binding Sites	Total Target Genes	Induced Target Genes
WRKY18	1403	1290	380
WRKY40	1622	1478	1477
WRKY33	1208	1140	1104

1077

Gene ID	Gene name	Score ChIP			Gene Product Description
		W18	W40	W33	
AT3G21630	<i>CERK1</i>	22.5	29.5	30.4	chitin elicitor receptor kinase 1
AT3G16030	<i>CES101</i>	56.2	56.2	23.8	lectin receptor kinase CES101
AT4G23130	<i>CRK5</i>	16.2	17.8	-	cysteine-rich receptor-like protein kinase 5
AT4G23220	<i>CRK14</i>	63.1	66.1	34.6	cysteine-rich receptor-like protein kinase 14
AT4G23250	<i>CRK17</i>	23.6	34.3	16.6	cysteine-rich receptor-like protein kinase 17
AT4G23260	<i>CRK18</i>	21.1	23.2	11.3	cysteine-rich receptor-like protein kinase 18
AT4G23280	<i>CRK20</i>	31.2	44.6	-	putative cysteine-rich receptor-like protein kinase 20
AT4G21400	<i>CRK28</i>	22.9	21.5	23.7	cysteine-rich receptor-like protein kinase 28
AT5G46330	<i>FLS2</i>	36.0	36.0	22.6	LRR receptor like kinase
AT2G39660	<i>BIK1</i>	23.8	30.7	-	serine/threonine-protein kinase BIK1
AT5G48380	<i>BIR1</i>	21.5	25.5	20.4	leucine-rich repeat receptor-like protein kinase
AT4G34390	<i>XLG2</i>	19.3	18.6	17.5	extra-large GTP-binding protein 2
AT4G34460	<i>AGB1</i>	10.8	-	16.3	guanine nucleotide-binding protein subunit beta
AT2G28830	<i>PUB12</i>	29.1	38.1	11.3	plant U-box 24 protein
AT4G18710	<i>BIN2</i>	26.3	26.0	16.1	Shaggy-related protein kinase eta
AT5G47910	<i>RBOHD</i>	-	12.3	-	respiratory burst oxidase-D
AT2G19190	<i>FRK1</i>	12.7	17.5	14.5	flag22 induced receptor kinase 1
AT5G48410	<i>GLR1.3</i>	-	-	20.8	glutamate receptor 1.3
AT5G11210	<i>GLR2.5</i>	12.1	-	14.2	glutamate receptor 2.5
AT2G29120	<i>GLR2.7</i>	16.3	20.3	-	glutamate receptor 2.7
AT2G29100	<i>GLR2.9</i>	-	18.8	20.7	glutamate receptor 2.9
AT5G01560	<i>LECRKA4.3</i>	20.8	25.6	-	Lectin-domain containing receptor kinase A4.3
AT2G17120	<i>LYM2</i>	32.3	44.2	-	LysM domain-containing GPI-anchored protein 2
AT1G73080	<i>PEPR1</i>	32.7	33.9	18.0	LRR receptor-like protein kinase PEPR1
AT5G64890	<i>PROPEP2</i>	18.9	20.3	21.2	elicitor peptide 2
AT5G64905	<i>PROPEP3</i>	26.1	35.0	40.3	elicitor peptide 3
AT1G09970	<i>RLK7</i>	13.0	15.2	16.3	leucine-rich receptor-like protein kinase LRR XI-23
AT2G02220	<i>PSKR1</i>	-	-	24.0	phytosulfokin receptor 1
AT2G38310	<i>PYL4</i>	13.4	16.6	-	abscisic acid receptor PYL4
AT1G65790	<i>RK1</i>	-	19.1	11.6	receptor kinase 1
AT1G65800	<i>RK2</i>	30.5	34.1	-	receptor kinase 2
AT4G21380	<i>RK3</i>	20.0	25.3	14.5	receptor kinase 3
AT5G60900	<i>RLK1</i>	37.8	43.8	15.5	receptor-like protein kinase 1
AT1G16150	<i>WAKL4</i>	30.6	35.9	20.2	wall associated kinase-like 4
AT1G16160	<i>WAKL5</i>	20.2	21.1	16.3	wall-associated receptor kinase-like 5

1079

1080 **Table 2:** Selected receptor and receptor-related target genes of WRKY18, WRKY40 and
1081 WRKY33. Indicated are ChIP scores for the respective WRKY factor and target gene at 2 h flg22
1082 treatment. - , indicates ChIP scores below the threshold level.

1083
1084
1085
1086

Gene ID	Gene name	Score ChIP			Gene Product Description
		W18	W40	W33	
AT1G73500	<i>MKK9</i>	28.9	26.3	-	MAP kinase kinase 9
AT1G01480	<i>ACS2</i>	27.3	36.4	-	1-aminocyclopropane-1-carboxylate synthase 2
AT4G11280	<i>ACS6</i>	60.9	90.0	29.9	1-aminocyclopropane-1-carboxylate synthase 6
AT4G37770	<i>ACS8</i>	23.4	22.3	30.5	1-aminocyclopropane-1-carboxylate synthase 8
AT1G62380	<i>ACO2</i>	18.6	12.5	-	aminocyclopropanecarboxylate oxidase
AT2G25490	<i>EBF1</i>	33.8	35.0	-	EIN3-binding F-box protein 1
AT5G25350	<i>EBF2</i>	73.4	67.7	22.8	EIN3-binding F-box protein 2
AT5G03280	<i>EIN2</i>	39.6	40.6	-	ethylene-insensitive protein 2
AT4G17500	<i>ERF-1</i>	54.0	65.7	41.1	ethylene-responsive transcription factor 1A
AT3G23240	<i>ERF1</i>	21.8	20.9	-	ethylene-responsive transcription factor 1B
AT5G47220	<i>ERF2</i>	15.4	17.4	-	ethylene-responsive transcription factor 2
AT3G15210	<i>ERF4</i>	16.2	22.3	-	ethylene-responsive transcription factor 4
AT5G47230	<i>ERF5</i>	-	15.3	24.2	ethylene-responsive transcription factor 5
AT4G17490	<i>ERF6</i>	21.5	23.2	-	ethylene-responsive transcription factor 6
AT1G06160	<i>ORA59</i>	21.8	22.5	-	ethylene-responsive transcr. factor ERF094
AT5G64750	<i>ABR1</i>	65.7	82.4	17.2	ethylene-responsive transcription factor ABR1
AT1G18570	<i>MYB51</i>	19.2	40.6	26.8	myb domain protein 51

1087

1088
1089
1090

1091

Table 3: Selected ET pathway-related target genes of WRKY18, WRKY40 and WRKY33. Indicated are ChIP scores for the respective WRKY factor and target gene at 2h flg22 treatment. - , indicates ChIP scores below the threshold level.

Gene ID	Gene name	Score ChIP			Gene Product Description
		W18	W40	W33	
AT1G74710	<i>ICS1</i>	51.0	75.0	-	isochorismate sythase 1
AT3G48090	<i>EDS1</i>	26.1	24.9	-	enhanced disease susceptibility 1 protein
AT4G39030	<i>EDS5</i>	27.5	32.5	11.5	enhanced disease susceptibility 5, drug transport.
AT1G02450	<i>NIMIN1</i>	18.9	20.5	-	protein NIM1-interacting 1
AT4G16890	<i>SNC1</i>	17.4	19.3	15.9	protein SUPPRESS. OF npr1-1, CONSTITUT. 1
AT5G45110	<i>NPR3</i>	-	14.2	-	NPR1-like protein 3
AT4G19660	<i>NPR4</i>	-	14.9	-	NPR1-like protein 4
AT5G13320	<i>PBS3</i>	47.4	44.2	-	auxin-responsive GH3 family protein
AT5G14930	<i>SAG101</i>	-	-	21.2	senescence-associated protein 101
AT2G47190	<i>MYB2</i>	-	15.9	-	myb domain protein 2
AT3G61250	<i>MYB17</i>	15.1	-	-	myb domain protein 17
AT1G74650	<i>MYB31</i>	41.5	51.8	-	myb domain protein 31
AT1G18570	<i>MYB51</i>	19.2	40.6	26.8	myb domain protein 51
AT1G68320	<i>MYB62</i>	21.3	-	-	myb domain protein 62
AT5G62470	<i>MYB96</i>	40.7	48.2	-	myb domain protein 96
AT5G65790	<i>MYB68</i>	26.8	30.1	-	myb domain protein 68
AT4G31800	<i>WRKY18</i>	229.4	97.6	21.1	WRKY transcription factor 18
AT5G24110	<i>WRKY30</i>	24.0	26.0	25.2	WRKY DNA-binding protein 30
AT5G22570	<i>WRKY38</i>	21.9	22.7	12.5	putative WRKY transcription factor 38
AT4G23810	<i>WRKY53</i>	14.9	18.2	29.5	putative WRKY transcription factor 53
AT2G25000	<i>WRKY60</i>	78.2	62.5	-	putative WRKY transcription factor 60
AT5G01900	<i>WRKY62</i>	-	12.5	-	putative WRKY transcription factor 62

Table 4: Selected SA pathway-related target genes of WRKY18, WRKY40 and WRKY33.

Indicated are ChIP scores for the respective WRKY factor and target gene at 2h flg22 treatment. - , indicates ChIP scores below the threshold level.

1097

Gene ID	Gene name	Score ChIP			Gene Product Description
		W18	W40	W33	
AT1G72450	<i>JAZ6</i>	30.4	30.9	38.6	jasmonate-zim-domaine protein 6, or AT1g72460
AT1G17420	<i>LOX3</i>	28.5	30.4	-	lipoxygenase 3
AT3G25780	<i>AOC3</i>	-	10.3	10.1	allene oxide cyclase 3
AT1G15520	<i>PDR12</i>	23.1	32.3	21.5	ABC transporter G family member 40
AT2G41370	<i>BOP2</i>	17.6	19.9	10.4	ankyrin repeat and BTB/POZ domain-cont. protein
AT1G06160	<i>ORA59</i>	14.2	12.2	-	ethylene-responsive transcription factor ERF094
AT5G26170	<i>WRKY50</i>	-	14.6	-	putative WRKY transcription factor 50
AT5G64810	<i>WRKY51</i>	19.2	22.1	15.8	putative WRKY transcription factor 51

1098

1099 **Table 5:** Selected JA pathway-related target genes of WRKY18, WRKY40 and WRKY33.
1100 Indicated are ChIP scores for the respective WRKY factor and target gene at 2 h flg22 treatment.
1101 - , indicates ChIP scores below the threshold level.

1102

1103

Gene ID	Gene name	Score ChIP			Gene Product Description
		W18	W40	W33	
AT4G30530	<i>GGP1</i>	yes	yes	yes	gamma-glutamyl-peptidase 1
AT1G02930	<i>GSTF6</i>	16.9	18.1	19.2	glutathione S-transferase 6
AT2G30860	<i>GSTF9</i>	-	-	11.9	glutathione S-transferase 9
AT4G31500	<i>CYP83B1</i>	yes	yes	16.1	Cytochrome P450 83B1
AT4G39950	<i>CYP79B2</i>	19.5	25.1	23.1	tryptophan N-hydroxylase 1
AT5G57220	<i>CYP81F2</i>	31.0	43.4	15.0	cytochrome P450 81F2
AT2G30770	<i>CYP71A13</i>	yes	yes	yes	cytochrome P450 71A13
AT2G30750	<i>CYP71A12</i>	yes	14.1	20.7	cytochrome P450 71A12
AT3G26830	<i>PAD3</i>	28.4	36.2	27.8	cytochrome P450 71B15
AT3G11820	<i>PEN1</i>	19.1	18.5	14.7	syntaxin-121, vesicle traffic
AT2G44490	<i>PEN2</i>	38.9	31.7	36.4	beta-glucosidase 26
AT1G59870	<i>PEN3</i>	107.2	137.8	64.7	ABC transporter G family member 36
AT1G18570	<i>MYB51</i>	19.2	40.6	26.8	myb domain protein 51
AT4G17490	<i>ERF6</i>	21.5	23.2	-	ethylene-responsive transcript. factor 6
AT1G21100	<i>IGMT1</i>	25.0	24.1	15.1	O-methyltransferase-like protein
AT1G21110	<i>IGMT3</i>	18.7	17.0	10.4	O-methyltransferase family protein
AT1G21120	<i>IGMT2</i>	22.5	25.4	17.2	O-methyltransferase family protein
AT1G21130	<i>IGMT4</i>	31.4	37.3	11.8	O-methyltransferase-like protein

1104

1105 **Table 6:** Selected target genes of WRKY18, WRKY40 and WRKY33 associated with indole
1106 glucosinolate and camalexin. Indicated are ChIP scores for the respective WRKY factor and
1107 target gene at 2 h flg22 treatment. Manual inspection of the binding sites in the IGV browser
1108 identified additional targets that were included (and marked with yes, compare Supplemental
1109 Fig.1). - , indicates ChIP scores below the threshold level.

1110

1111

TF families	WRKY18	WRKY40	WRKY33	Genome
total TFs	129 / 10.0% **	156 / 10.5% **	102 / 9,0% **	1700 / 5.6%
AP2/ERF	27 / 19.6% **	34 / 24.6% **	13 / 9.4% *	138
NAC	6 / 6.3%	8 / 8.3%	5 / 5.2%	96
MYB	12 / 9.2% *	14 / 10.7% *	12 / 9.2% *	131
bHLH	10 / 6.2%	12 / 7.5%	7 / 4.3%	161
WRKY	22/ 30.6% **	27 / 37.5% **	20 / 27.8% **	72

1112

1113 **Table 7:** WRKY18, WRKY40 and WRKY33 binding to genes from selected TF families related to
1114 stress response at 2 h flg22 treatment. Indicated are the numbers of gene loci of a TF gene family
1115 bound by the respective WRKY factor and their fraction in percent of the entire TF gene family.
1116 Single and double asterisks indicate $p < 0.05$ and $p < 0.0001$, respectively, in a hypergeometric
1117 test for enrichment. The column “Genome” lists the total numbers of genes within the Arabidopsis
1118 genome (*agris*, <http://arabidopsis.med.ohio-state.edu/AtTFDB/>).

1119

1120

1121

Genotype	Total	Up	Down
WT	6892	4099	2793
<i>wrky18</i>	7208	4244	2964
<i>wrky40</i>	7222	4230	2992
<i>wrky18 wrky40</i>	7297	4179	3118

1122

1123 **Table 8:** Numbers of genes altered in their expression in the respective genotype upon flg22
1124 treatment. Indicated are the total numbers of genes with altered expression, and numbers of up-
1125 and down-regulated genes (absolute FC \geq 2, FDR < 0.05) at 2 h flg22.

1126

1127

Genotype	Total	0 h			2 h	
		Up	Down		Up	Down
<i>wrky18</i>	3	0	3		6	3
<i>wrky40</i>	15	12	3		108	96
<i>wrky18 wrky40</i>	112	92	20		426	259

1128

1129 **Table 9:** Numbers of differentially expressed genes (DEGs) in the respective genotype compared
1130 to WT. Indicated are the total numbers of DEGs, and numbers of up- and down-regulated genes
1131 (absolute FC ≥ 2, FDR < 0.05) at 0 h and 2 h flg22.

1132

1133

Binding TF	DEGs In	DRTs		
		Total	Up	Down
WRKY18	<i>wrky18</i>	4	2	2
WRKY40	<i>wrky40</i>	58	55	3
WRKY18	<i>wrky18 wrky40</i>	122	112	10
WRKY40	<i>wrky18 wrky40</i>	131	119	12
WRKY18 and WRKY40	<i>wrky18 wrky40</i>	119	109	10

1134

1135 **Table 10:** Directly regulated target genes (DRTs) at 2h flg22 of WRKY18 or/and WRKY40 in
1136 *wrky18*, *wrky40*, and *wrky18 wrky40*. DRTs are defined as differentially expressed genes (DEGs)
1137 in the respective genotype that are directly bound by the indicated WRKY TF. Shown are the total
1138 numbers and the numbers of up- and down-regulated DRT genes.

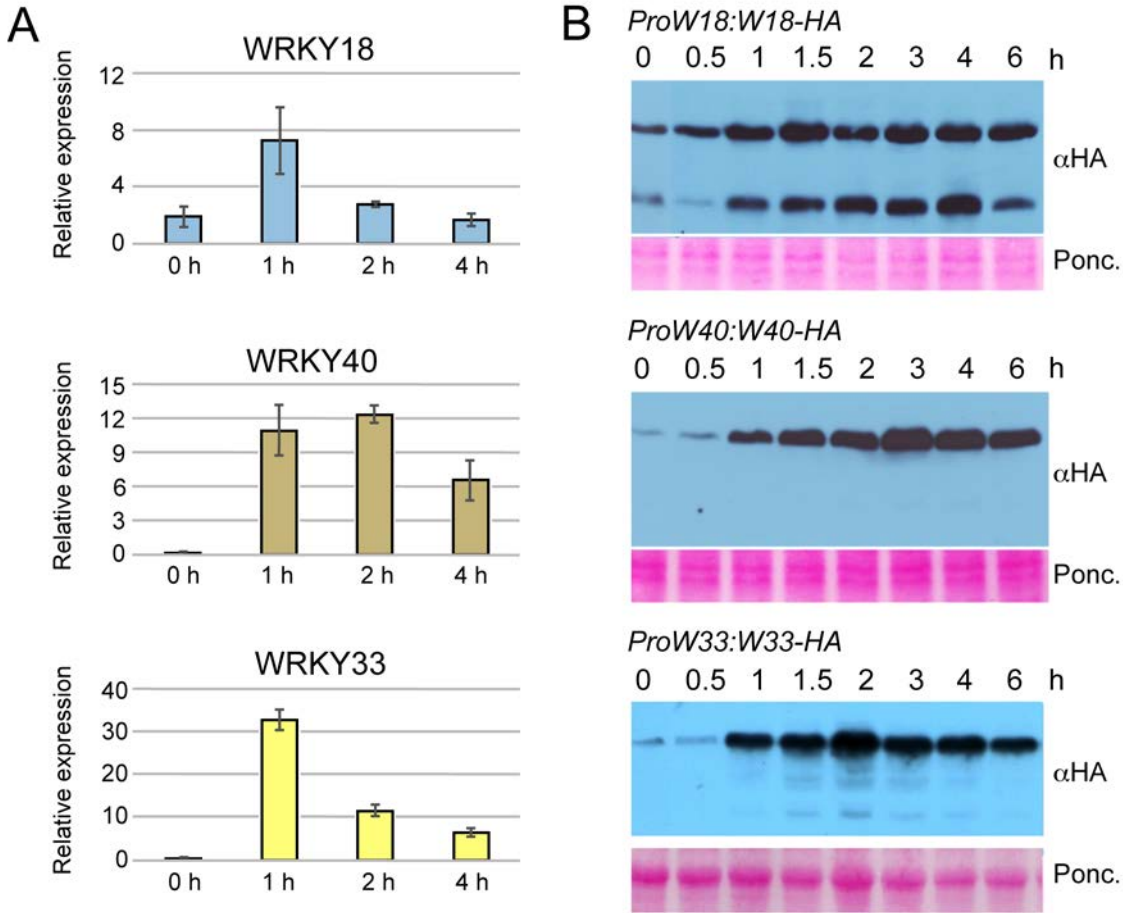


Figure 1. Induction of *WRKY18*, *WRKY40* and *WRKY33* by flg22 treatment. **A.** RT-qPCR analysis of flg22-induced RNA levels. Total RNA was isolated from seedlings treated for 0, 1, 2 and 4 h with flg22 and analyzed by qPCR using gene-specific primers. Shown are the mean and standard deviation (error bars) calculated from three biological replicates. **B.** Immunoblot analysis of flg22-induced protein levels. Protein extracts from seedlings of the HA-tagged complementation lines were treated for indicated times with flg22 and subsequently analyzed by immunoblot using an anti-HA antibody. Ponceau S staining served as loading control.

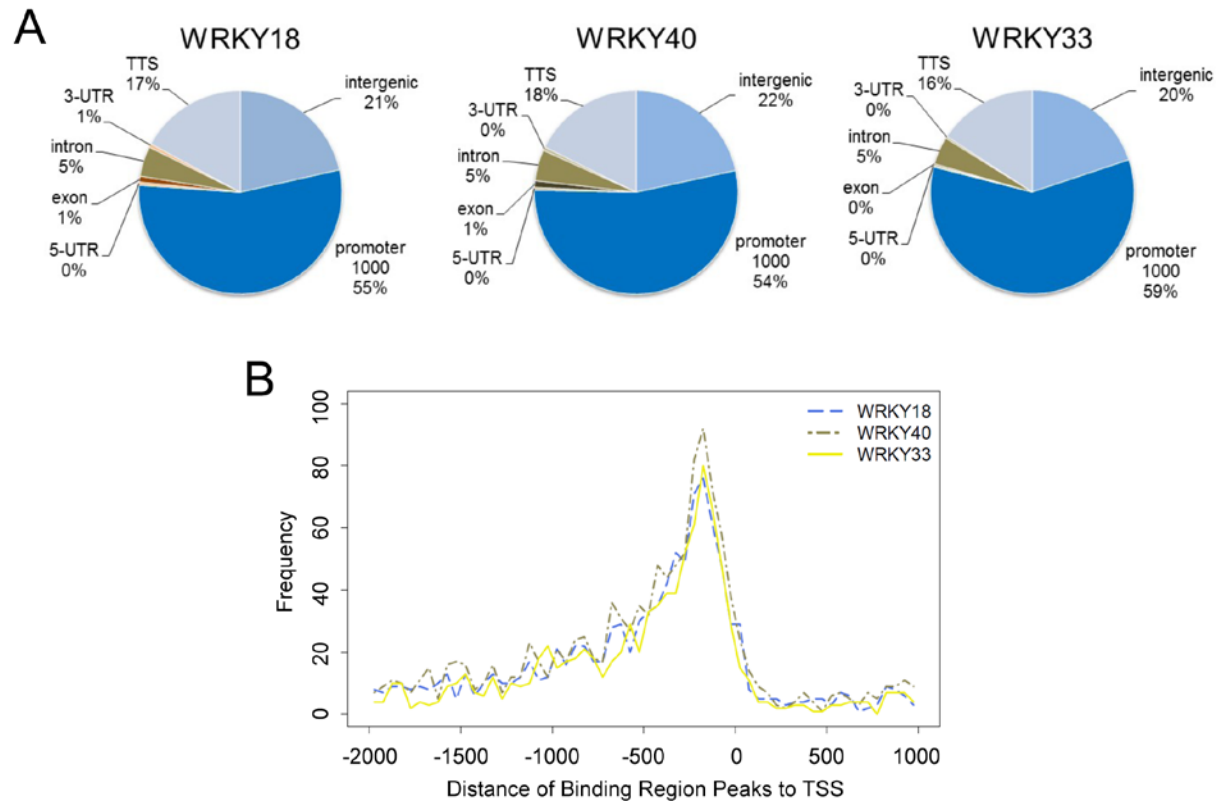


Figure 2. Distribution of flg22-induced WRKY18, WRKY40 and WRKY33 binding regions in the Arabidopsis genome. A. Prevalence of WRKY binding regions in different genomic categories. Promoters are defined as the 1000-bp region upstream of the transcription start site (TSS). Transcription termination site (TTS) refers to the 1000-bp region downstream of the 3'UTR, and genome regions located in between a TTS and the promoter of the next gene are regarded as intergenic. B. Distance of WRKY binding region peaks to the transcription start site. The number of binding region peaks for each 50-bp region relative to the TSS is indicated.

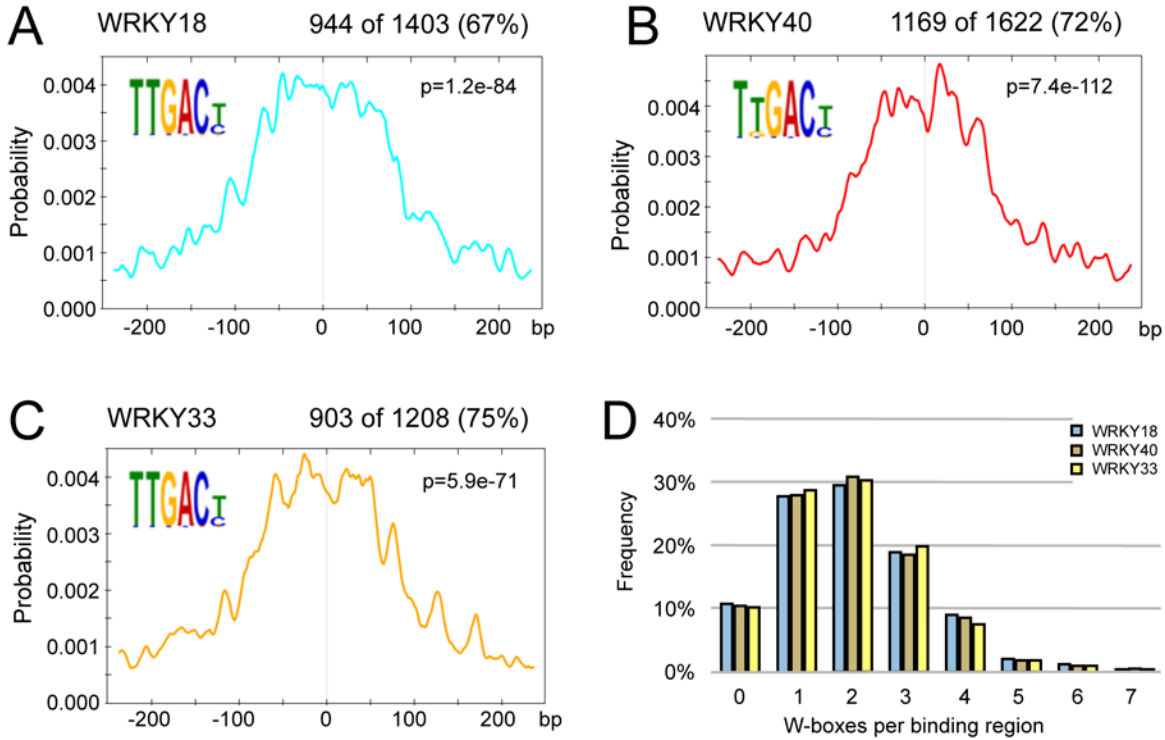


Figure 3. The W-box is the predominant motif within WRKY binding regions. A, B, C. Motif position probability graphs for WRKY18 (A), WRKY40 (B) and WRKY33 (C) established by CentriMo motif search (Bailey and Machanick, 2012). Indicated is the most frequent motif, its rate of occurrence, and the probability of this motif occurring at a given position relative to the binding peak summit (0) in the 500-bp binding regions. The included p-value describes the significance for central enrichment. D. Distribution of W-box abundances in WRKY18, WRKY40 and WRKY33 binding regions.

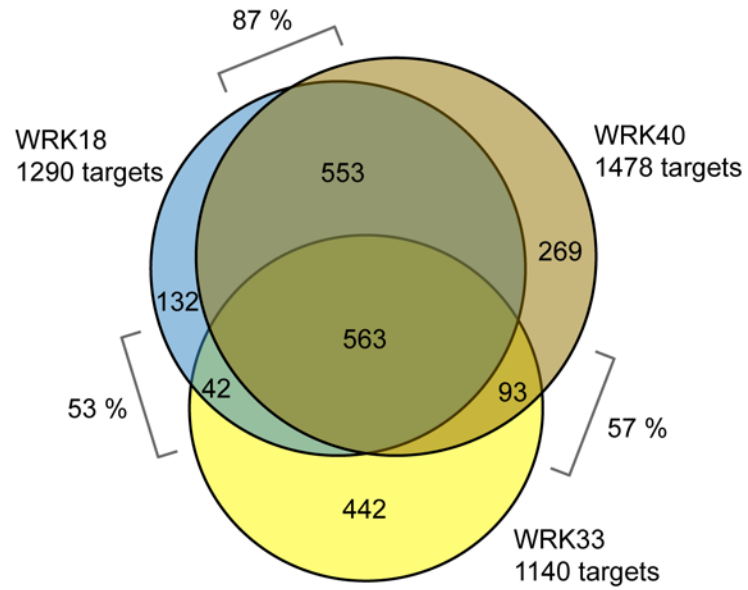


Figure 4. Overlap of WRKY18, WRKY40 and WRKY33 target gene sets after 2 h flg22 treatment. Indicated are the number of target genes in each section, and the fraction of overlapping genes between each pair of WRKY target gene sets with respect to the smaller set.

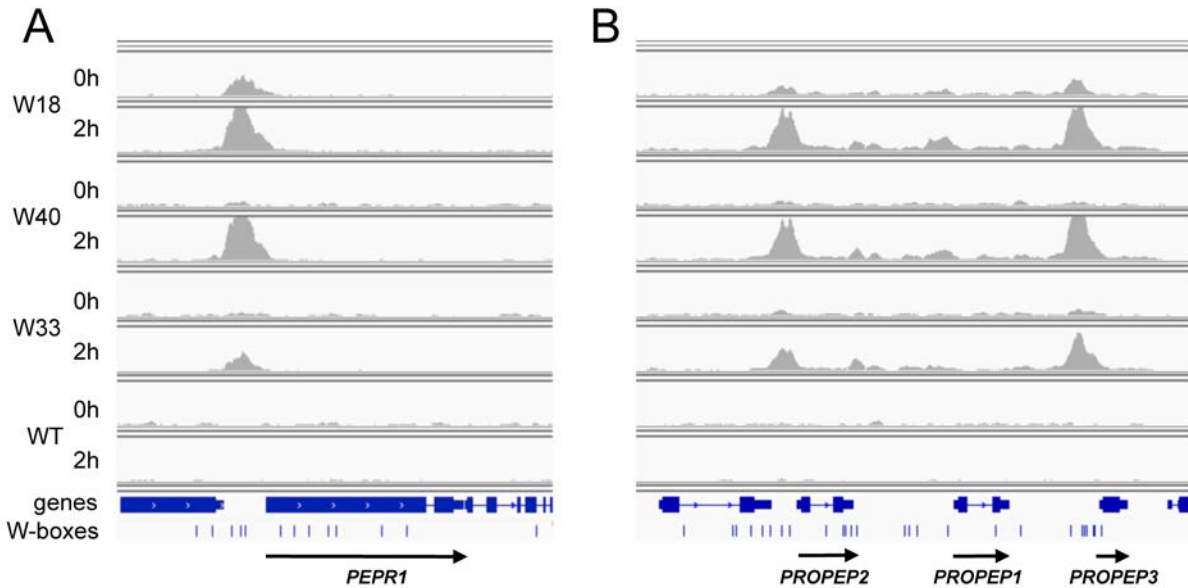


Figure 5. WRKY18, WRKY40 and WRKY33 binding to the *PEPR1*, *PROPEP2* and *PROPEP3* loci. A. Integrative Genome Viewer (IGV) images of the *PEPR1* (A) and *PROPEP1-3* loci (B). Binding of WRKYs is visualized by read coverage histograms indicating sequencing read accumulation before (0 h) or after flg22 treatment (2 h). WT samples served as negative control. The three lower tracks show the corresponding gene structures, position of W-boxes and the direction of transcription (arrows).

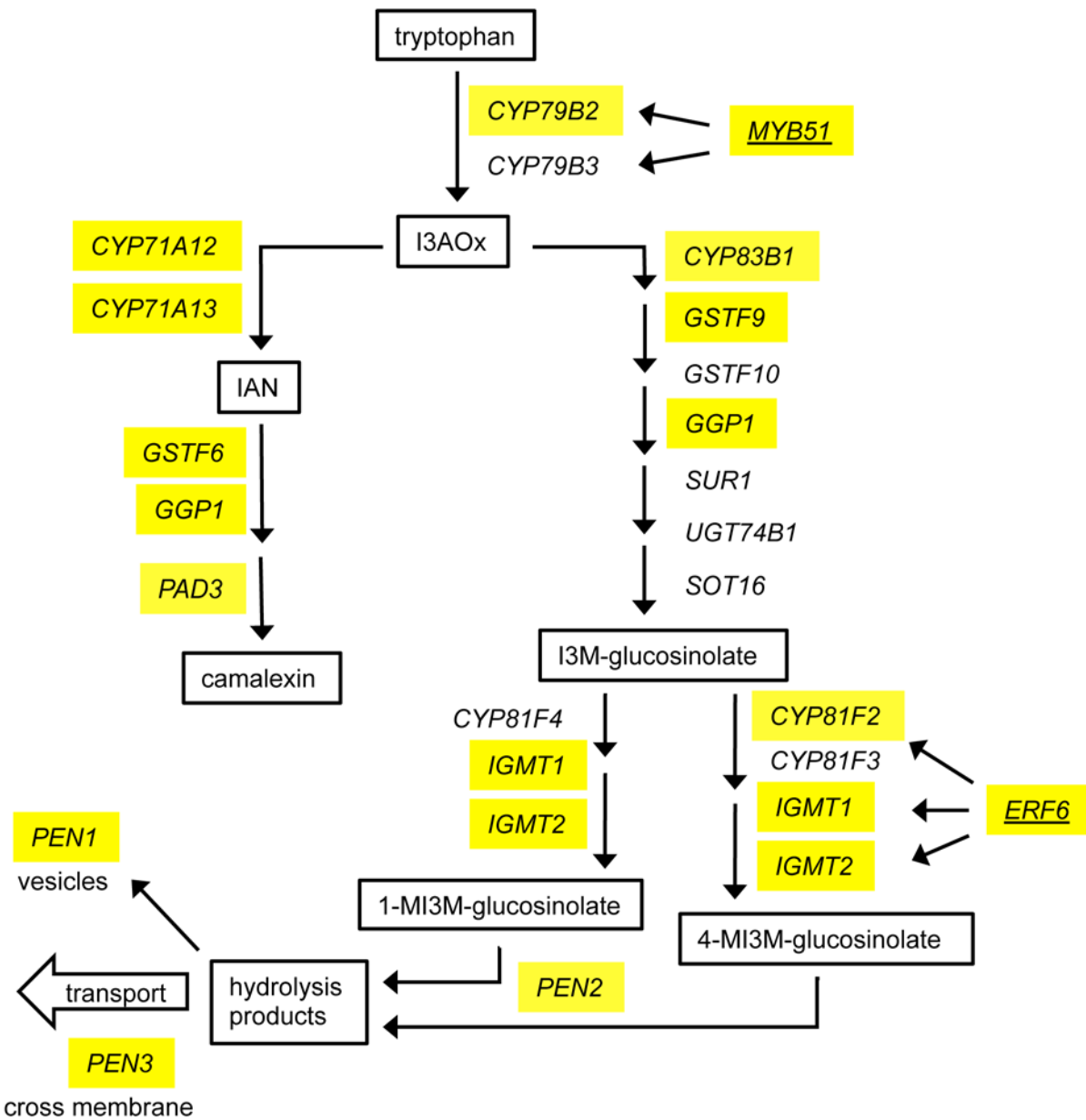


Figure 6. WRKY18, WRKY40 and WRKY33 bind to genes involved in biosynthesis and transport of secondary metabolites camalexin and indole-glucosinolates (biosynthetic pathways adapted from Sonderby et al., 2010; Pfalz et al., 2011; Morldrup et al., 2013). Identified WRKY18, WRKY40 or WRKY33 target genes are indicated in yellow. TFs are underlined.

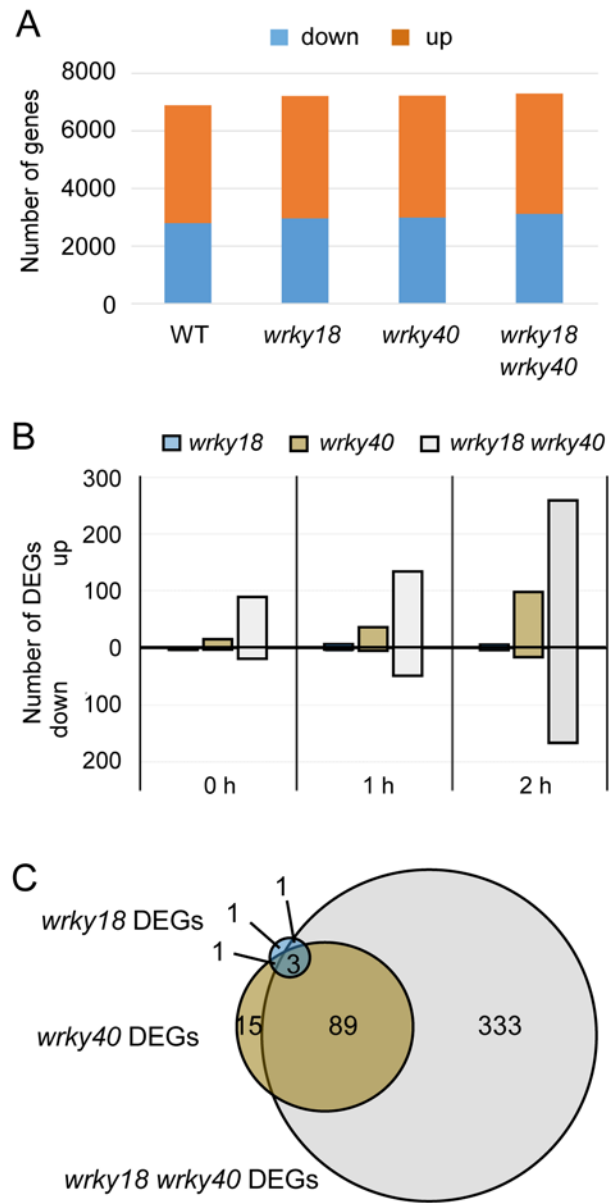


Figure 7. Differentially expressed genes in *wrky18*, *wrky40*, and *wrky18 wrky40* plants. A. Number of significantly ($FC \geq 2$, $FDR < 0.05$) up- or down-regulated genes at 2 h flg22 treatment compared to 0 h in the indicated genotype. B. Number of up- and down-regulated, differentially expressed genes (DEGs) ($FDR < 0.05$, $FC \geq 2$) in the respective mutant lines compared to WT at 0, 1, or 2 h post flg22 treatment. C. Overlap of the identified sets of DEGs in the respective mutant lines relative to WT at 2 h post flg22 treatment. Indicated are the number of DEGs in each section.

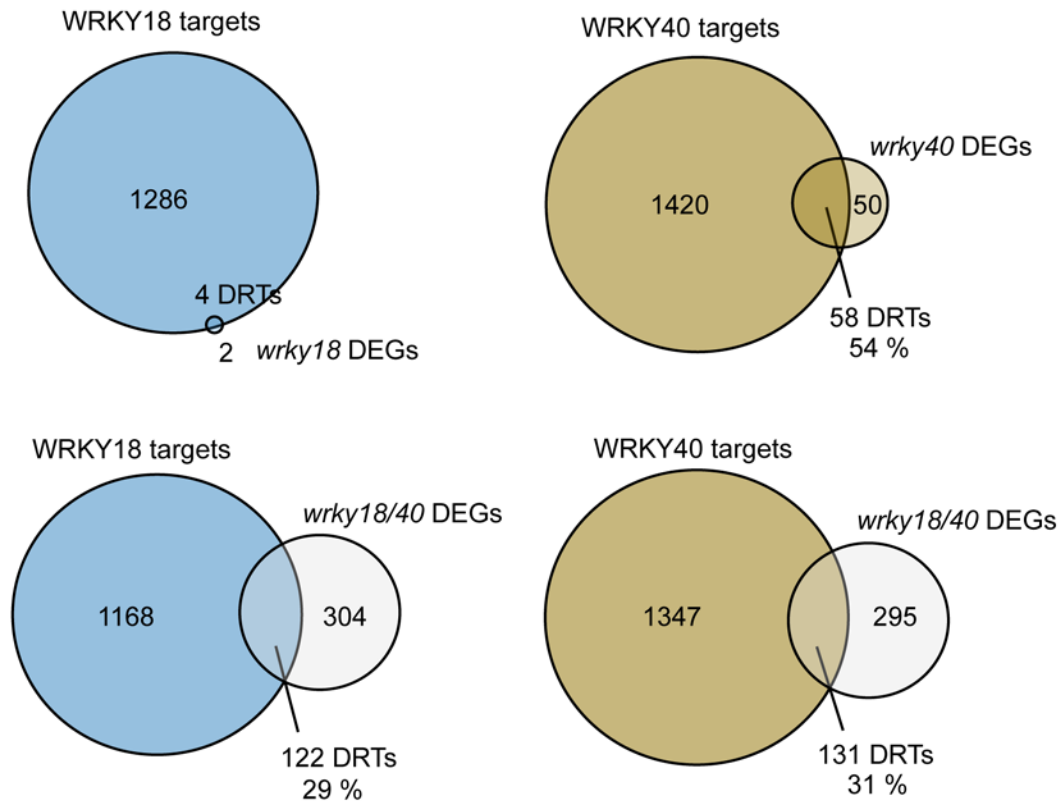


Figure 8. Directly regulated target genes (DRTs) of WRKY18 and WRKY40. DRTs were identified by the overlaps of the WRKY18 and WRKY40 target gene sets with the sets of differentially expressed genes (DEGs) compared to WT in *wrky18*, *wrky40* and *wrky18 wrky40* mutants at 2 h post flg22 treatment. Indicated are the number of target genes, DEGs and DRTs in the respective sections, and the fraction DEGs identified as DRTs in each comparison.

Parsed Citations

Albert, M. (2013). Peptides as triggers of plant defence. *J. Exp. Bot.* 64, 5269-5279.

Pubmed: [Author and Title](#)

CrossRef: [Author and Title](#)

Google Scholar: [Author Only](#) [Title Only](#) [Author and Title](#)

Alonso, J.M., Hirayama, T., Roman, G., Nourizadeh, S., and Ecker, J.R. (1999). EIN2, a bifunctional transducer of ethylene and stress responses in *Arabidopsis*. *Science* 284, 2148-2152.

Pubmed: [Author and Title](#)

CrossRef: [Author and Title](#)

Google Scholar: [Author Only](#) [Title Only](#) [Author and Title](#)

Anders, S., Pyl, P.T., and Huber, W. (2015). HTSeq—a Python framework to work with high-throughput sequencing data. *Bioinformatics* 31, 166-169.

Pubmed: [Author and Title](#)

CrossRef: [Author and Title](#)

Google Scholar: [Author Only](#) [Title Only](#) [Author and Title](#)

Assaad, F.F., Qiu, J.-L., Youngs, H., Ehrhardt, D., Zimmerli, L., Kalde, M., Wanner, G., Peck, S.C., Edwards, H., Ramonell, K., Somerville, C.R., and Thordal-Christensen, H. (2004). The PEN1 syntaxin defines a novel cellular compartment upon fungal attack and is required for the timely assembly of papillae. *Mol. Biol. Cell* 15, 5118-5129.

Pubmed: [Author and Title](#)

CrossRef: [Author and Title](#)

Google Scholar: [Author Only](#) [Title Only](#) [Author and Title](#)

Bailey, T.L. (2011). DREME: motif discovery in transcription factor ChIP-seq data. *Bioinformatics* 27, 1653-1659.

Pubmed: [Author and Title](#)

CrossRef: [Author and Title](#)

Google Scholar: [Author Only](#) [Title Only](#) [Author and Title](#)

Bailey, T.L., and Machanick, P. (2012). Inferring direct DNA binding from ChIP-seq. *Nucleic Acids Res.* 40, e128.

Pubmed: [Author and Title](#)

CrossRef: [Author and Title](#)

Google Scholar: [Author Only](#) [Title Only](#) [Author and Title](#)

Bak, S., Beisson, F., Bishop, G., Hamberger, B., Höfer, R., Paquette, S., and Werck-Reichhart, D. (2011). Cytochromes P450. *The Arabidopsis Book*, e0144.

Pubmed: [Author and Title](#)

CrossRef: [Author and Title](#)

Google Scholar: [Author Only](#) [Title Only](#) [Author and Title](#)

Bartels, S., and Boller, T. (2015). Quo vadis, Pep? Plant elicitor peptides at the crossroads of immunity, stress, and development. *J. Exp. Bot.* 66, 5183-5193.

Pubmed: [Author and Title](#)

CrossRef: [Author and Title](#)

Google Scholar: [Author Only](#) [Title Only](#) [Author and Title](#)

Birkenbihl, R.P., Diezel, C., and Somssich, I.E. (2012). *Arabidopsis* WRKY33 is a key transcriptional regulator of hormone and metabolic responses towards *Botrytis cinerea* infection. *Plant Physiol.* 159, 266-285.

Pubmed: [Author and Title](#)

CrossRef: [Author and Title](#)

Google Scholar: [Author Only](#) [Title Only](#) [Author and Title](#)

Broekgaarden, C., Caarls, L., Vos, I.A., Pieterse, C.M.J., and Van Wees, S.C.M. (2015). Ethylene: Traffic controller on hormonal crossroads to defense. *Plant Physiol.* 169, 2371-2379.

Pubmed: [Author and Title](#)

CrossRef: [Author and Title](#)

Google Scholar: [Author Only](#) [Title Only](#) [Author and Title](#)

Canet, J.V., Dobón, A., Fajmonová, J., and Tornero, P. (2012). The BLADE-ON-PETIOLE genes of *Arabidopsis* are essential for resistance induced by methyl jasmonate. *BMC Plant Biol* 12, 199.

Pubmed: [Author and Title](#)

CrossRef: [Author and Title](#)

Google Scholar: [Author Only](#) [Title Only](#) [Author and Title](#)

Cecchini, N.M., Jung, H.W., Engle, N.L., Tschaplinski, T.J., and Greenberg, J.T. (2014). ALD1 regulates basal immune components and early inducible defense responses in *Arabidopsis*. *Mol. Plant-Microbe Interact.* 28, 455-466.

Pubmed: [Author and Title](#)

CrossRef: [Author and Title](#)

Google Scholar: [Author Only](#) [Title Only](#) [Author and Title](#)

Chi, Y., Yang, Y., Zhou, Y., Zhou, J., Fan, B., Yu, J.-Q., and Chen, Z. (2013). Protein-protein interactions in the regulation of WRKY transcription factors. *Mol. Plant* 6, 287-300.

Pubmed: [Author and Title](#)

CrossRef: [Author and Title](#)

Google Scholar: [Author Only](#) [Title Only](#) [Author and Title](#)

Chini, A., Fonseca, S., Fernandez, G., Adie, B., Chico, J.M., Lorenzo, O., Garcia-Casado, G., Lopez-Vidriero, I., Lozano, F.M., Ponce, M.R., Micol, J.L., and Solano, R. (2007). The JAZ family of repressors is the missing link in jasmonate signalling. *Nature* 448, 666-

671.

Pubmed: [Author and Title](#)
CrossRef: [Author and Title](#)
Google Scholar: [Author Only](#) [Title Only](#) [Author and Title](#)

Choura, M., Rebai, A., and Masmoudi, K. (2015). Unraveling the WRKY transcription factors network in Arabidopsis thaliana by integrative approach. Network Biol. 5, 55-61.

Pubmed: [Author and Title](#)
CrossRef: [Author and Title](#)
Google Scholar: [Author Only](#) [Title Only](#) [Author and Title](#)

Clay, N.K., Adio, A.M., Denoux, C., Jander, G., and Ausubel, F.M. (2009). Glucosinolate metabolites required for an Arabidopsis innate immune response. Science 323, 95-101.

Pubmed: [Author and Title](#)
CrossRef: [Author and Title](#)
Google Scholar: [Author Only](#) [Title Only](#) [Author and Title](#)

Czechowski, T., Stitt, M., Altmann, T., Udvardi, M.K., and Scheible, W.-R. (2005). Genome-wide identification and testing of superior reference genes for transcript normalization in Arabidopsis. Plant Physiol. 139, 5-17.

Pubmed: [Author and Title](#)
CrossRef: [Author and Title](#)
Google Scholar: [Author Only](#) [Title Only](#) [Author and Title](#)

Eulgem, T. (2006). Dissecting the WRKY web of plant defense regulators. PLoS Pathog. 2, e126.

Pubmed: [Author and Title](#)
CrossRef: [Author and Title](#)
Google Scholar: [Author Only](#) [Title Only](#) [Author and Title](#)

Eulgem, T., and Somssich, I.E. (2007). Networks of WRKY transcription factors in defense signaling. Curr. Opin. Plant Biol. 10, 366-371.

Pubmed: [Author and Title](#)
CrossRef: [Author and Title](#)
Google Scholar: [Author Only](#) [Title Only](#) [Author and Title](#)

Felix, G., Duran, J.D., Volko, S., and Boller, T. (1999). Plants have a sensitive perception system for the most conserved domain of bacterial flagellin. Plant J. 18, 265-276.

Pubmed: [Author and Title](#)
CrossRef: [Author and Title](#)
Google Scholar: [Author Only](#) [Title Only](#) [Author and Title](#)

Frerigmann, H., and Gigolashvili, T. (2014). MYB34, MYB51, and MYB122 distinctly regulate indolic glucosinolate biosynthesis in Arabidopsis thaliana. Mol. Plant 7, 814-828.

Pubmed: [Author and Title](#)
CrossRef: [Author and Title](#)
Google Scholar: [Author Only](#) [Title Only](#) [Author and Title](#)

Fu, Z.Q., Yan, S., Saleh, A., Wang, W., Ruble, J., Oka, N., Mohan, R., Spoel, S.H., Tada, Y., Zheng, N., and Dong, X. (2012). NPR3 and NPR4 are receptors for the immune signal salicylic acid in plants. Nature 486, 228-232.

Pubmed: [Author and Title](#)
CrossRef: [Author and Title](#)
Google Scholar: [Author Only](#) [Title Only](#) [Author and Title](#)

Gagne, J.M., Smalle, J., Gingerich, D.J., Walker, J.M., Yoo, S.-D., Yanagisawa, S., and Vierstra, R.D. (2004). Arabidopsis EIN3-binding F-box 1 and 2 form ubiquitin-protein ligases that repress ethylene action and promote growth by directing EIN3 degradation. Proc. Natl. Acad. Sci. USA 101, 6803-6808.

Pubmed: [Author and Title](#)
CrossRef: [Author and Title](#)
Google Scholar: [Author Only](#) [Title Only](#) [Author and Title](#)

Gao, M., Wang, X., Wang, D., Xu, F., Ding, X., Zhang, Z., Bi, D., Cheng, Y.T., Chen, S., Li, X., and Zhang, Y. (2009). Regulation of cell death and innate immunity by two receptor-like kinases in Arabidopsis. Cell Host Microbe 6, 34-44.

Pubmed: [Author and Title](#)
CrossRef: [Author and Title](#)
Google Scholar: [Author Only](#) [Title Only](#) [Author and Title](#)

Gao, Q.-M., Venugopal, S., Navarre, D., and Kachroo, A. (2011). Low oleic acid-derived repression of jasmonic acid-inducible defense responses requires the WRKY50 and WRKY51 proteins. Plant Physiol. 155, 464-476.

Pubmed: [Author and Title](#)
CrossRef: [Author and Title](#)
Google Scholar: [Author Only](#) [Title Only](#) [Author and Title](#)

Garcion, C., Lohmann, A., Lamodièrre, E., Catinot, J., Buchala, A., Doermann, P., and Metraux, J.-P. (2008). Characterization and biological function of the ISOCHORISMATE SYNTHASE2 gene of Arabidopsis. Plant Physiol. 147, 1279-1287.

Pubmed: [Author and Title](#)
CrossRef: [Author and Title](#)
Google Scholar: [Author Only](#) [Title Only](#) [Author and Title](#)

Gendrel, A.-V., Lippman, Z., Martienssen, R., and Colot, V. (2005). Profiling histone modification patterns in plants using genomic tiling microarrays. Nat. Meth. 2, 213-218.

Pubmed: [Author and Title](#)

CrossRef: [Author and Title](#)
Google Scholar: [Author Only](#) [Title Only](#) [Author and Title](#)

Grant, C.E., Bailey, T.L., and Noble, W.S. (2011). FIMO: scanning for occurrences of a given motif. Bioinformatics 27.

Pubmed: [Author and Title](#)
CrossRef: [Author and Title](#)
Google Scholar: [Author Only](#) [Title Only](#) [Author and Title](#)

Heinz, S., Benner, C., Spann, N., Bertolino, E., Lin, Y.C., Laslo, P., Cheng, J.X., Murre, C., Singh, H., and Glass, C.K. (2010). Simple combinations of lineage-determining transcription factors prime cis-regulatory elements required for macrophage and B cell identities. Mol. Cell 38, 576-589.

Pubmed: [Author and Title](#)
CrossRef: [Author and Title](#)
Google Scholar: [Author Only](#) [Title Only](#) [Author and Title](#)

Heyndrickx, K.S., de Velde, J.V., Wang, C., Weigel, D., and Vandepoele, K. (2014). A functional and evolutionary perspective on transcription factor binding in Arabidopsis thaliana. Plant Cell 26, 3894-3910.

Pubmed: [Author and Title](#)
CrossRef: [Author and Title](#)
Google Scholar: [Author Only](#) [Title Only](#) [Author and Title](#)

Hou, S., Wang, X., Chen, D., Yang, X., Wang, M., Turrà, D., Di Pietro, A., and Zhang, W. (2014). The secreted peptide PIP1 amplifies immunity through receptor-like kinase 7. PLoS Pathog. 10, e1004331.

Pubmed: [Author and Title](#)
CrossRef: [Author and Title](#)
Google Scholar: [Author Only](#) [Title Only](#) [Author and Title](#)

Huang, P.-Y., Catinot, J., and Zimmerli, L. (2016). Ethylene response factors in Arabidopsis immunity. J. Exp. Bot. 67, 1231-1241.

Pubmed: [Author and Title](#)
CrossRef: [Author and Title](#)
Google Scholar: [Author Only](#) [Title Only](#) [Author and Title](#)

Huot, B., Yao, J., Montgomery, B.L., and He, S.Y. (2014). Growth-defense tradeoffs in plants: a balancing act to optimize fitness. Mol. Plant 7, 1267-1287.

Pubmed: [Author and Title](#)
CrossRef: [Author and Title](#)
Google Scholar: [Author Only](#) [Title Only](#) [Author and Title](#)

Jing, Y., and Lin, R. (2015). The VQ motif-containing protein family of plant-specific transcriptional regulators. Plant Physiol. 169, 371-378.

Pubmed: [Author and Title](#)
CrossRef: [Author and Title](#)
Google Scholar: [Author Only](#) [Title Only](#) [Author and Title](#)

Kadota, Y., Sklenar, J., Derbyshire, P., Stransfeld, L., Asai, S., Ntoukakis, V., Jones, Jonathan D., Shirasu, K., Menke, F., Jones, A., and Zipfel, C. (2014). Direct Regulation of the NADPH Oxidase RBOHD by the PRR-Associated Kinase BIK1 during Plant Immunity. Mol. Cell 54, 43-55.

Pubmed: [Author and Title](#)
CrossRef: [Author and Title](#)
Google Scholar: [Author Only](#) [Title Only](#) [Author and Title](#)

Law, C., Chen, Y., Shi, W., and Smyth, G. (2014). voom: precision weights unlock linear model analysis tools for RNA-seq read counts. Genome Biol. 15, R29.

Pubmed: [Author and Title](#)
CrossRef: [Author and Title](#)
Google Scholar: [Author Only](#) [Title Only](#) [Author and Title](#)

Li, B., Meng, X., Shan, L., and He, P. (2016). Transcriptional regulation of pattern-triggered immunity in plants. Cell Host Microbe 19, 641-650.

Pubmed: [Author and Title](#)
CrossRef: [Author and Title](#)
Google Scholar: [Author Only](#) [Title Only](#) [Author and Title](#)

Li, G., Meng, X., Wang, R., Mao, G., Han, L., Liu, Y., and Zhang, S. (2012). Dual-level regulation of ACC synthase activity by MPK3/MPK6 cascade and its downstream WRKY transcription factor during ethylene induction in Arabidopsis. PLoS Genet. 8, e1002767.

Pubmed: [Author and Title](#)
CrossRef: [Author and Title](#)
Google Scholar: [Author Only](#) [Title Only](#) [Author and Title](#)

Li, R., Zhang, J., Li, J., Zhou, G., Wang, Q., Bian, W., Erb, M., and Lou, Y. (2015). Prioritizing plant defence over growth through WRKY regulation facilitates infestation by non-target herbivores. eLIFE 4, e04805.

Pubmed: [Author and Title](#)
CrossRef: [Author and Title](#)
Google Scholar: [Author Only](#) [Title Only](#) [Author and Title](#)

Li, X., Clarke, J.D., Zhang, Y., and Dong, X. (2001). Activation of an EDS1-mediated R-gene pathway in the snc1 mutant leads to constitutive, NPR1-independent pathogen resistance. Mol. Plant-Microbe Interact. 14, 1131-1139.

Pubmed: [Author and Title](#)
CrossRef: [Author and Title](#)
Google Scholar: [Author Only](#) [Title Only](#) [Author and Title](#)

Liang, X., Ding, P., Lian, K., Wang, J., Ma, M., Li, L., Li, L., Li, M., Zhang, X., Chen, S., Zhang, Y., and Zhou, J.-M. (2016). Arabidopsis heterotrimeric G proteins regulate immunity by directly coupling to the FLS2 receptor. eLife 5, e13568.

Pubmed: [Author and Title](#)

CrossRef: [Author and Title](#)

Google Scholar: [Author Only](#) [Title Only](#) [Author and Title](#)

Liu, S., Kracher, B., Ziegler, J., Birkenbihl, R.P., and Somssich, I.E. (2015). Negative regulation of ABA signaling by WRKY33 is critical for Arabidopsis immunity towards Botrytis cinerea 2100. eLIFE 4, e07295.

Pubmed: [Author and Title](#)

CrossRef: [Author and Title](#)

Google Scholar: [Author Only](#) [Title Only](#) [Author and Title](#)

Livak, K.J., and Schmittgen, T.D. (2001). Analysis of relative gene expression data using real-time quantitative PCR and the 2(-Delta Delta C(T)) Method. Methods 25, 402-408.

Pubmed: [Author and Title](#)

CrossRef: [Author and Title](#)

Google Scholar: [Author Only](#) [Title Only](#) [Author and Title](#)

Logemann, E., Birkenbihl, R.P., Rawat, V., Schneeberger, K., Schmelzer, E., and Somssich, I.E. (2013). Functional dissection of the PROPEP2 and PROPEP3 promoters reveals the importance of WRKY factors in mediating microbe-associated molecular pattern-induced expression. New Phytol. 198, 1165-1177.

Pubmed: [Author and Title](#)

CrossRef: [Author and Title](#)

Google Scholar: [Author Only](#) [Title Only](#) [Author and Title](#)

Lozano-Durán, R., Macho, A.P., Boutrot, F., Segonzac, C., Somssich, I.E., and Zipfel, C. (2013). The transcriptional regulator BZR1 mediates trade-off between plant innate immunity and growth. eLife 2, e00983.

Pubmed: [Author and Title](#)

CrossRef: [Author and Title](#)

Google Scholar: [Author Only](#) [Title Only](#) [Author and Title](#)

Lu, D., Lin, W., Gao, X., Wu, S., Cheng, C., Avila, J., Heese, A., Devarenne, T.P., He, P., and Shan, L. (2011). Direct ubiquitination of pattern recognition receptor FLS2 attenuates plant innate immunity. Science 332, 1439-1442.

Pubmed: [Author and Title](#)

CrossRef: [Author and Title](#)

Google Scholar: [Author Only](#) [Title Only](#) [Author and Title](#)

Lu, K., Liang, S., Wu, Z., Bi, C., Yu, Y.-T., Wang, X.-F., and Zhang, D.-P. (2016). Overexpression of an Arabidopsis cysteine-rich receptor-like protein kinase, CRK5, enhances abscisic acid sensitivity and confers drought tolerance. J. Exp. Bot. 67, 5009-5027.

Pubmed: [Author and Title](#)

CrossRef: [Author and Title](#)

Google Scholar: [Author Only](#) [Title Only](#) [Author and Title](#)

Machanick, P., and Bailey, T. (2011). MEME-ChIP: motif analysis of large DNA datasets. Bioinformatics 27, 1696 - 1697.

Pubmed: [Author and Title](#)

CrossRef: [Author and Title](#)

Google Scholar: [Author Only](#) [Title Only](#) [Author and Title](#)

Macho, A.P., and Zipfel, C. (2014). Plant PRRs and the activation of innate immune signaling. Mol. Cell 54.

Pubmed: [Author and Title](#)

CrossRef: [Author and Title](#)

Google Scholar: [Author Only](#) [Title Only](#) [Author and Title](#)

Mao, G., Meng, X., Liu, Y., Zheng, Z., Chen, Z., and Zhang, S. (2011). Phosphorylation of a WRKY Transcription Factor by Two Pathogen-Responsive MAPKs Drives Phytoalexin Biosynthesis in Arabidopsis. Plant Cell 23, 1639-1653.

Pubmed: [Author and Title](#)

CrossRef: [Author and Title](#)

Google Scholar: [Author Only](#) [Title Only](#) [Author and Title](#)

Monaghan, J., and Zipfel, C. (2012). Plant pattern recognition receptor complexes at the plasma membrane. Curr. Opin. Plant Biol. 15, 1-9.

Pubmed: [Author and Title](#)

CrossRef: [Author and Title](#)

Google Scholar: [Author Only](#) [Title Only](#) [Author and Title](#)

Møldrup, M.E., Salomonsen, B., Geu-Flores, F., Olsen, C.E., and Halkier, B.A (2013). De novo genetic engineering of the camalexin biosynthetic pathway. J. Biotechnol. 167, 296-301.

Pubmed: [Author and Title](#)

CrossRef: [Author and Title](#)

Google Scholar: [Author Only](#) [Title Only](#) [Author and Title](#)

Navarro, L., Zipfel, C., Rowland, O., Keller, I., Robatzek, S., Boller, T., and Jones, J.D.G. (2004). The transcriptional innate immune response to flg22. Interplay and overlap with avr gene-dependent defense responses and bacterial pathogenesis. Plant Physiol. 135, 1113-1128.

Pubmed: [Author and Title](#)

CrossRef: [Author and Title](#)

Google Scholar: [Author Only](#) [Title Only](#) [Author and Title](#)

Newman, M.-A., Sundelin, T., Nielsen, J.T., and Erbs, G. (2013). MAMP (Microbe-Associated Molecular Pattern) triggered immunity

in *Plants. Front. Plant Sci.* 4, 139.

Pubmed: [Author and Title](#)

CrossRef: [Author and Title](#)

Google Scholar: [Author Only](#) [Title Only](#) [Author and Title](#)

Okrent, R.A., Brooks, M.D., and Wildermuth, M.C. (2009). Arabidopsis GH3.12 (PBS3) conjugates amino acids to 4-substituted benzoates and is inhibited by salicylate. J. Biol. Chem. 284, 9742-9754.

Pubmed: [Author and Title](#)

CrossRef: [Author and Title](#)

Google Scholar: [Author Only](#) [Title Only](#) [Author and Title](#)

Pandey, G.K., Grant, J.J., Cheong, Y.H., Kim, B.G., Li, L., and Luan, S. (2005). ABR1, an APETALA2-domain transcription factor that functions as a repressor of ABA response in Arabidopsis. Plant Physiol. 139, 1185-1193.

Pubmed: [Author and Title](#)

CrossRef: [Author and Title](#)

Google Scholar: [Author Only](#) [Title Only](#) [Author and Title](#)

Pandey, S.P., Roccaro, M., Schön, M., Logemann, E., and Somssich, I.E. (2010). Transcriptional reprogramming regulated by WRKY18 and WRKY40 facilitates powdery mildew infection of Arabidopsis. Plant J. 64, 912-923.

Pubmed: [Author and Title](#)

CrossRef: [Author and Title](#)

Google Scholar: [Author Only](#) [Title Only](#) [Author and Title](#)

Pfalz, M., Mikkelsen, M.D., Bednarek, P., Olsen, C.E., Halkier, B.A., and Kroymann, J. (2011). Metabolic engineering in *Nicotiana benthamiana* reveals key enzyme functions in Arabidopsis indole glucosinolate modification. Plant Cell 23, 716-729.

Pubmed: [Author and Title](#)

CrossRef: [Author and Title](#)

Google Scholar: [Author Only](#) [Title Only](#) [Author and Title](#)

Pieterse, C.M.J., Van der Does, D., Zamioudis, C., Leon-Reyes, A., and Van Wees, S.C.M. (2012). Hormonal modulation of plant immunity. Annu. Rev. Cell. Dev. Biol. 28, 489-521.

Pubmed: [Author and Title](#)

CrossRef: [Author and Title](#)

Google Scholar: [Author Only](#) [Title Only](#) [Author and Title](#)

Pré, M., Atallah, M., Champion, A., De Vos, M., Pieterse, C.M.J., and Memelink, J. (2008). The AP2/ERF domain transcription factor ORA59 integrates jasmonic acid and ethylene signals in plant defense. Plant Physiol. 147, 1347-1357.

Pubmed: [Author and Title](#)

CrossRef: [Author and Title](#)

Google Scholar: [Author Only](#) [Title Only](#) [Author and Title](#)

Qiu, J.-L., Fiil, B.-K., Petersen, K., Nielsen, H.B., Botanga, C.J., Thorgrimsen, S., Palma, K., Suarez-Rodriguez, M.C., Sandbech-Clausen, S., Lichota, J., Brodersen, P., Grasser, K.D., Mattsson, O., Glazebrook, J., Mundy, J., and Petersen, M. (2008). Arabidopsis MAP kinase 4 regulates gene expression through transcription factor release in the nucleus. EMBO J. 27, 2214-2221.

Pubmed: [Author and Title](#)

CrossRef: [Author and Title](#)

Google Scholar: [Author Only](#) [Title Only](#) [Author and Title](#)

Robert-Seilantantz, A., Grant, M., and Jones, J.D.G. (2011). Hormone crosstalk in plant disease and defense: More than just JASMONATE-SALICYLATE antagonism. Annu. Rev. Phytopathol. 49, 317-343.

Pubmed: [Author and Title](#)

CrossRef: [Author and Title](#)

Google Scholar: [Author Only](#) [Title Only](#) [Author and Title](#)

Robinson, M.D., McCarthy, D.J., and Smyth, G.K. (2010). edgeR: a Bioconductor package for differential expression analysis of digital gene expression data. Bioinformatics 26, 139-140.

Pubmed: [Author and Title](#)

CrossRef: [Author and Title](#)

Google Scholar: [Author Only](#) [Title Only](#) [Author and Title](#)

Rushton, P.J., Somssich, I.E., Ringler, P., and Shen, Q.J. (2010). WRKY transcription factors. Trends Plant Sci. 15, 247-258.

Pubmed: [Author and Title](#)

CrossRef: [Author and Title](#)

Google Scholar: [Author Only](#) [Title Only](#) [Author and Title](#)

Schön, M., Töller, A., Diezel, C., Roth, C., Westphal, L., Wiermer, M., and Somssich, I.E. (2013). Analyses of wrky18 wrky40 plants reveal critical roles of SA/EDS1 signaling and indole-glucosinolate biosynthesis for *Golovinomyces orontii* resistance and a loss-of resistance towards *Pseudomonas syringae* pv. tomato AvrRPS4. Mol. Plant-Microbe Interact. 26, 758-767.

Pubmed: [Author and Title](#)

CrossRef: [Author and Title](#)

Google Scholar: [Author Only](#) [Title Only](#) [Author and Title](#)

Schweizer, F., Bodenhausen, N., Lassueur, S., Masclaux, F.G., and Reymond, P. (2013). Differential contribution of transcription factors to Arabidopsis thaliana defence against *Spodoptera littoralis*. Front. Plant Sci. 4, 13.

Pubmed: [Author and Title](#)

CrossRef: [Author and Title](#)

Google Scholar: [Author Only](#) [Title Only](#) [Author and Title](#)

Schwessinger, B., and Ronald, P.C. (2012). Plant innate immunity: perception of conserved microbial signatures. Annu. Rev. Plant Biol. 63, 451-482.

Pubmed: [Author and Title](#)
CrossRef: [Author and Title](#)
Google Scholar: [Author Only](#) [Title Only](#) [Author and Title](#)

Serrano, M., Wang, B., Aryal, B., Garcion, C., Abou-Mansour, E., Heck, S., Geisler, M., Mauch, F., Nawrath, C., and Métraux, J.-P. (2013). Export of salicylic acid from the chloroplast requires the multidrug and toxin extrusion-like transporter EDS5. *Plant Physiol.* 162, 1815-1821.

Pubmed: [Author and Title](#)
CrossRef: [Author and Title](#)
Google Scholar: [Author Only](#) [Title Only](#) [Author and Title](#)

Shankaranarayanan, P., Mendoza-Parra, M.-A., Walia, M., Wang, L., Li, N., Trindade, L.M., and Gronemeyer, H. (2011). Single-tube linear DNA amplification (LinDA) for robust ChIP-seq. *Nat. Meth.* 8, 565-567.

Pubmed: [Author and Title](#)
CrossRef: [Author and Title](#)
Google Scholar: [Author Only](#) [Title Only](#) [Author and Title](#)

Shen, Q.-H., Saijo, Y., Mauch, S., Biskup, C., Bieri, S., Keller, B., Seki, H., Ulker, B., Somssich, I.E., and Schulze-Lefert, P. (2007). Nuclear activity of MLA immune receptors links isolate-specific and basal disease-resistance responses. *Science* 315, 1098-1103.

Pubmed: [Author and Title](#)
CrossRef: [Author and Title](#)
Google Scholar: [Author Only](#) [Title Only](#) [Author and Title](#)

Sønderby, I.E., Geu-Flores, F., and Halkier, B.A. (2010). Biosynthesis of glucosinolates - gene discovery and beyond. *Trends Plant Sci.* 15, 283-290.

Pubmed: [Author and Title](#)
CrossRef: [Author and Title](#)
Google Scholar: [Author Only](#) [Title Only](#) [Author and Title](#)

Song, J.T., Lu, H., McDowell, J.M., and Greenberg, J.T. (2004). A key role for ALD1 in activation of local and systemic defenses in *Arabidopsis*. *Plant J.* 40, 200-212.

Pubmed: [Author and Title](#)
CrossRef: [Author and Title](#)
Google Scholar: [Author Only](#) [Title Only](#) [Author and Title](#)

Song, L., Huang, S.-s.C., Wise, A., Castanon, R., Nery, J.R., Chen, H., Watanabe, M., Thomas, J., Bar-Joseph, Z., and Ecker, J.R. (2016). A transcription factor hierarchy defines an environmental stress response network. *Science* 354, 598.

Pubmed: [Author and Title](#)
CrossRef: [Author and Title](#)
Google Scholar: [Author Only](#) [Title Only](#) [Author and Title](#)

Sun, T., Zhang, Y., Li, Y., Zhang, Q., Ding, Y., and Zhang, Y. (2015). ChIP-seq reveals broad roles of SARD1 and CBP60g in regulating plant immunity. *Nat. Commun.* 6, 10159.

Pubmed: [Author and Title](#)
CrossRef: [Author and Title](#)
Google Scholar: [Author Only](#) [Title Only](#) [Author and Title](#)

Sun, Y., Li, L., Macho, A.P., Han, Z., Hu, Z., Zipfel, C., Zhou, J.-m., and Chai, J. (2013). Structural basis for flg22-induced activation of the *Arabidopsis* FLS2-BAK1 immune complex. *Science* 342, 224-628.

Pubmed: [Author and Title](#)
CrossRef: [Author and Title](#)
Google Scholar: [Author Only](#) [Title Only](#) [Author and Title](#)

Tena, G., Boudsocq, M., and Sheen, J. (2011). Protein kinase signaling networks in plant innate immunity. *Curr. Opin. Plant Biol.* 14, 519-529.

Pubmed: [Author and Title](#)
CrossRef: [Author and Title](#)
Google Scholar: [Author Only](#) [Title Only](#) [Author and Title](#)

Thorvaldsdóttir, H., Robinson, J.T., and Mesirov, J.P. (2013). Integrative Genomics Viewer (IGV): high-performance genomics data visualization and exploration. *Briefings in Bioinformatics* 14, 178-192.

Pubmed: [Author and Title](#)
CrossRef: [Author and Title](#)
Google Scholar: [Author Only](#) [Title Only](#) [Author and Title](#)

Truman, W., and Glazebrook, J. (2012). Co-expression analysis identifies putative targets for CBP60g and SARD1 regulation. *BMC Plant Biol* 12, 216.

Pubmed: [Author and Title](#)
CrossRef: [Author and Title](#)
Google Scholar: [Author Only](#) [Title Only](#) [Author and Title](#)

Tsuda, K., and Somssich, I.E. (2015). Transcriptional networks in plant immunity. *New Phytol.* 206, 932-947.

Pubmed: [Author and Title](#)
CrossRef: [Author and Title](#)
Google Scholar: [Author Only](#) [Title Only](#) [Author and Title](#)

Tsuda, K., Sato, M., Stoddard, T., Glazebrook, J., and Katagiri, F. (2009). Network properties of robust immunity in plants. *PLoS Genet.* 5, e1000772.

Pubmed: [Author and Title](#)
CrossRef: [Author and Title](#)
Google Scholar: [Author Only](#) [Title Only](#) [Author and Title](#)

Valouev, A., Johnson, D.S., Sundquist, A., Medina, C., Anton, E., Batzoglou, S., Myers, R.M., and Sidow, A. (2008). Genome-wide analysis of transcription factor binding sites based on ChIP-Seq data. Nat. Meth. 5, 829-834.

Pubmed: [Author and Title](#)

CrossRef: [Author and Title](#)

Google Scholar: [Author Only](#) [Title Only](#) [Author and Title](#)

Vidhyasekaran, P. (2014). PAMP signaling in plant innate immunity. In PAMP Signals in Plant Innate Immunity - Signal Perception and Transduction (Springer), pp. 17-161.

Pubmed: [Author and Title](#)

CrossRef: [Author and Title](#)

Google Scholar: [Author Only](#) [Title Only](#) [Author and Title](#)

Wan, J., Zhang, X.-C., Neece, D., Ramonell, K.M., Clough, S., Kim, S.-y., Stacey, M.G., and Stacey, G. (2008). A LysM receptor-like kinase plays a critical role in chitin signaling and fungal resistance in Arabidopsis. Plant Cell 20, 471-481.

Pubmed: [Author and Title](#)

CrossRef: [Author and Title](#)

Google Scholar: [Author Only](#) [Title Only](#) [Author and Title](#)

Wang, X., Gao, J., Zhu, Z., Dong, X., Wang, X., Ren, G., Zhou, X., and Kuai, B. (2015). TCP transcription factors are critical for the coordinated regulation of ISOCHORISMATE SYNTHASE 1 expression in Arabidopsis thaliana. Plant J. 82, 151-162.

Pubmed: [Author and Title](#)

CrossRef: [Author and Title](#)

Google Scholar: [Author Only](#) [Title Only](#) [Author and Title](#)

Weigel, R.R., Pfitzner, U.M., and Gatz, C. (2005). Interaction of NIMIN1 with NPR1 modulates PR gene expression in Arabidopsis. Plant Cell 17, 1279-1291.

Pubmed: [Author and Title](#)

CrossRef: [Author and Title](#)

Google Scholar: [Author Only](#) [Title Only](#) [Author and Title](#)

Widemann, E., Miesch, L., Lugan, R., Holder, E., Heinrich, C., Aubert, Y., Miesch, M., Pinot, F., and Heitz, T. (2013). The amidohydrolases IAR3 and ILL6 contribute to jasmonoyl-isoleucine hormone turnover and generate 12-hydroxyjasmonic acid upon wounding in Arabidopsis leaves. J. Biol. Chem. 288, 31701-31714.

Pubmed: [Author and Title](#)

CrossRef: [Author and Title](#)

Google Scholar: [Author Only](#) [Title Only](#) [Author and Title](#)

Xu, J., Meng, J., Meng, X., Zhao, Y., Liu, J., Sun, T., Liu, Y., Wang, Q., and Zhang, S. (2016). Pathogen-responsive MPK3 and MPK6 reprogram the biosynthesis of indole glucosinolates and their derivatives in Arabidopsis immunity. Plant Cell 28, 1144-1162.

Pubmed: [Author and Title](#)

CrossRef: [Author and Title](#)

Google Scholar: [Author Only](#) [Title Only](#) [Author and Title](#)

Xu, X., Chen, C., Fan, B., and Chen, Z. (2006). Physical and functional interactions between pathogen-induced Arabidopsis WRKY18, WRKY40, and WRKY60 transcription factors. Plant Cell 18, 1310-1326.

Pubmed: [Author and Title](#)

CrossRef: [Author and Title](#)

Google Scholar: [Author Only](#) [Title Only](#) [Author and Title](#)

Yoo, S.-D., Cho, Y.-H., Tena, G., Xiong, Y., and Sheen, J. (2008). Dual control of nuclear EIN3 by bifurcate MAPK cascades in C2H4 signalling. Nature 451, 789-795.

Pubmed: [Author and Title](#)

CrossRef: [Author and Title](#)

Google Scholar: [Author Only](#) [Title Only](#) [Author and Title](#)

Zhang, X., Han, X., Shi, R., Yang, G., Qi, L., Wang, R., and Li, G. (2013). Arabidopsis cysteine-rich receptor-like kinase 45 positively regulates disease resistance to Pseudomonas syringae. Plant Physiol. Biochem. 73, 383-391.

Pubmed: [Author and Title](#)

CrossRef: [Author and Title](#)

Google Scholar: [Author Only](#) [Title Only](#) [Author and Title](#)

Zheng, X.-y., Zhou, M., Yoo, H., Pruneda-Paz, J.L., Spivey, N.W., Kay, S.A., and Dong, X. (2015). Spatial and temporal regulation of biosynthesis of the plant immune signal salicylic acid. Proc. Natl. Acad. Sci. USA 112, 9166-9173.

Pubmed: [Author and Title](#)

CrossRef: [Author and Title](#)

Google Scholar: [Author Only](#) [Title Only](#) [Author and Title](#)

Zheng, Z., Qamar, S.A., Chen, Z., and Mengiste, T. (2006). Arabidopsis WRKY33 transcription factor is required for resistance to necrotrophic fungal pathogens. Plant J. 48, 592-605.

Pubmed: [Author and Title](#)

CrossRef: [Author and Title](#)

Google Scholar: [Author Only](#) [Title Only](#) [Author and Title](#)

Zipfel, C., Robatzek, S., Navarro, L., Oakeley, E.J., Jones, J.D.G., Felix, G., and Boller, T. (2004). Bacterial disease resistance in Arabidopsis through flagellin perception. Nature 428, 764-767.

Pubmed: [Author and Title](#)

CrossRef: [Author and Title](#)

Google Scholar: [Author Only](#) [Title Only](#) [Author and Title](#)

Zipfel, C., Kunze, G., Chinchilla, D., Caniard, A., Jones, J.D.G., Boller, T., and Felix, G. (2006). Perception of the bacterial PAMP EF-

Tu by the receptor EFR restricts Agrobacterium-mediated transformation. Cell 125, 749-760.

Pubmed: [Author and Title](#)

CrossRef: [Author and Title](#)

Google Scholar: [Author Only](#) [Title Only](#) [Author and Title](#)

Induced Genome-Wide Binding of Three Arabidopsis WRKY Transcription Factors during Early MAMP-Triggered Immunity

Rainer P Birkenbihl, Barbara Kracher and Imre E. Somssich

Plant Cell; originally published online December 23, 2016;

DOI 10.1105/tpc.16.00681

This information is current as of April 27, 2017

Supplemental Data	http://www.plantcell.org/content/suppl/2016/12/23/tpc.16.00681.DC1.html http://www.plantcell.org/content/suppl/2017/02/06/tpc.16.00681.DC2.html
Permissions	https://www.copyright.com/ccc/openurl.do?sid=pd_hw1532298X&issn=1532298X&WT.mc_id=pd_hw1532298X
eTOCs	Sign up for eTOCs at: http://www.plantcell.org/cgi/alerts/ctmain
CiteTrack Alerts	Sign up for CiteTrack Alerts at: http://www.plantcell.org/cgi/alerts/ctmain
Subscription Information	Subscription Information for <i>The Plant Cell</i> and <i>Plant Physiology</i> is available at: http://www.aspb.org/publications/subscriptions.cfm